[American Journal of Science, Vol. 309, December, 2009, P. 958–984, DOI 10.2475/10.2009.02]

ANAEROBIC METHANE OXIDATION BY ARCHAEA/SULFATE-REDUCING BACTERIA AGGREGATES: 2. ISOTOPIC CONSTRAINTS

MARC J. ALPERIN*,† and TORI M. HOEHLER**

ABSTRACT. Recent studies employing novel analytical tools provide detailed, microscopic portraits of archaea/sulfate-reducing bacteria aggregates in sediments from methane seep and vent sites. One of the most striking features of these aggregates is that lipid and cell carbon are highly depleted in ^{13}C ($\delta^{13}C < -60‰$). Biogenic methane, with $\delta^{13}C$ values of -50 to -110 permil, is a logical candidate for carbon source of these aggregates. Accordingly, it is widely assumed that the archaea oxidize and assimilate methane, and that methane-derived carbon is transferred to the sulfate-reducing bacteria (SRB) symbionts as CO_2 or as a partially oxidized intermediate. However, methane is not the only possible source of ^{13}C-depleted carbon in archaea/SRB aggregates. ΣCO_2 in sediments at seep and vent sites tends to be isotopically "light" due to decomposition of organic matter derived from chemoautotrophic organisms. In addition, CO_2 is depleted in ^{13}C by ~10 permil compared to ΣCO_2 owing to the equilibrium isotope effect. Assimilation of this "light" CO_2 by methanogenic archaea and autotrophic SRB, combined with enzymatic isotope effects, could also yield lipid and biomass that are highly depleted in ^{13}C.

We derive general equations based on isotope mass-balance and calibrated with laboratory and field data to predict the isotopic composition of archaeal cell carbon and lipids derived from autotrophic methanogenesis and anaerobic methane oxidation. The calculations show that observed $\delta^{13}C$ values for archaeal biomass and lipids at methane seep and vent sites are readily accounted for by isotope fractionation during methane production from CO_2, and that biomass produced during anaerobic methane oxidation is only slightly depleted in ^{13}C relative to methane unless the enzymatic isotope effect associated with the anabolic arm of the assimilation-dissimilation branch point is considerably larger than the isotope effect associated with the catabolic arm. We also apply an isotope diffusion-reaction model to demonstrate that micro-gradients in $\delta^{13}C$-CO_2 cannot be maintained within archaea/SRB aggregates. However, ^{13}C-depleted carbon in SRB members of the aggregate is readily explained by autotrophic sulfate-reduction with bulk porewater CO_2 as carbon source.

These results illustrate that ^{13}C-depleted biomass and lipids observed in sediments from methane seep and vent sites may be derived from CO_2-reducing archaea and autotrophic sulfate-reducing bacteria. The inference of anaerobic methanotrophy based on ^{13}C depletion in archaeal and sulfate-reducing bacterial cell carbon and/or lipids should be considered tentative unless corroborated by independent, concordant evidence of net methane consumption.

INTRODUCTION

Anaerobic methane oxidation (AMO) is readily identified in many anoxic marine sediments by the curvature it imparts on the methane-depth distribution. For steady state, laterally homogenous sediments in which molecular diffusion is the dominant transport process, Fick's First Law and conservation of mass require upward concavity in the methane profile throughout the zone of net methane consumption. In these systems, temporal stability and relatively simple transport physics make it possible to test for concordance between independent indicators of methane oxidation. For

* Marine Sciences Department, University of North Carolina at Chapel Hill, Chapel Hill, North Carolina 27599-3300, USA; alperin@email.unc.edu

** NASA Ames Research Center, Mail Stop 239-4, Moffett Field, California 94035-1000, USA; tori.m.hoehler@nasa.gov

† Corresponding author

example, the methane-oxidation rate profile determined by radiotracers can be depth-integrated and checked for mass-balance with the net flux into the methane-oxidation zone predicted from the methane concentration profile. Furthermore, the depth of the methane-oxidation zone indicated by rate and concentration profiles can be compared to the region where δ^{13}C-CH_4 and δ^{2}H-CH_4 values shift due to the kinetic isotope effect during methane oxidation. Consistency between multiple indicators has been demonstrated in a number of studies (for example, Alperin and others, 1988; Martens and others, 1999; Thomsen and others, 2001) and provides unequivocal evidence of the existence, biogeochemical zonation, and magnitude of AMO at specific sites.

For sediments that harbor methane seeps and hydrothermal vents, it is not possible to identify net methane oxidation on the basis of methane concentration profiles. Rapid fluid advection creates complex and variable transport physics that cannot be readily parameterized. In addition, it is difficult to measure concentration profiles accurately because near-surface methane concentrations in seep/vent sediments exceed 10 mM (table 1) and cores are consequently disturbed by out-gassing during recovery. In these systems, AMO is often inferred on the basis of stable carbon isotope ratios in components of organic matter that are associated with anaerobic microorganisms (see table 1 for references).

Lipid biomarkers characteristic of methanogenic archaea, and highly depleted in the heavy isotope of carbon ($-58‰ \geq \delta^{13}C \geq -133‰$; table 1) have been discovered in sediments at methane seep and vent sites. In addition, aggregates composed of archaea and sulfate-reducing bacteria (SRB) have been observed that contain archaeal cells with δ^{13}C values as low as −96 permil (Orphan and others, 2001b). Biogenic methane, with δ^{13}C values of −50 to −110 permil (Whiticar, 1999), is the logical candidate for carbon source of these archaea. Consequently, archaeal lipids and/or biomass with δ^{13}C values < -60 permil are often taken to indicate anaerobic methanotrophy (see review by Hinrichs and Boetius, 2002). However, this interpretation could be complicated by autotrophic methanogens; these archaea are known to discriminate against ^{13}C during CO_2 reduction. Elvert and others (2000) recognize autotrophic methanogenesis as a possible source of "ultra-light" lipids in methane-seep sediments, but this mechanism has generally been discounted (Hinrichs and others, 1999; Pancost and others, 2000; Teske and others, 2002). However, a recent experimental study by Londry and others (2008) suggests that "there may be some overlap between the δ^{13}C of lipids produced by methanogenic and methanotrophic archaea" (p. 619).

Lipids and biomass isolated from methane seep and vent sites and attributed to SRB are also depleted in ^{13}C (for example, Hinrichs and others, 2000; Boetius and others, 2000; Werne and others, 2002; Orphan and others, 2001b). The carbon in these organic materials tends to be slightly enriched (by 10 to 30‰) in heavy isotope relative to that derived from archaea, but δ^{13}C values of −50 to −100 permil are common, and clearly implicate methane as a possible carbon source. One of the more popular explanations for the ^{13}C-depletion is that autotrophic SRB utilize inorganic carbon that is isotopically "light" compared to bulk CO_2 due to the close physical association between archaeal and bacterial cells in methane-oxidizing aggregates. This explanation requires that the CO_2 pool, with its relatively long residence time, maintain significant gradients in δ^{13}C over small spatial scales (several microns) where molecular diffusion is a rapid and effective mixing process.

Recent studies employing novel analytical tools have produced a wealth of insights regarding archaea/SRB aggregates at methane seep and vent sites (see review by Hinrichs and Boetius, 2002). Lipid biomarkers, as well as 16S ribosomal-RNA (rRNA) phylogeny, suggest that the archaea in these aggregates are related to methanogens.

Table 1

Environmental characteristics and isotopic composition of CH_4, CO_2, POC, and archaeal lipids in marine sediments at methane seep and hydrothermal vent sites[1]

Study site (environment)[2]	Temperature (ºC)	Water depth (m)	Bottom water	Biological community[3]	[CH_4] (mM)	δ^{13}C-CH_4 (‰)	δ^{13}C-CO_2 (‰)	δ^{13}C-POC (‰)	δ^{13}C-archaeal lipids[4] (‰) [depth interval]
Eel River Basin (ME, GH)	4	501 to 556	oxic	BM, CIC	85[5]	–35 to –63	–38[6]	–29	–76 to –108 [0 to 22]
Hydrate Ridge (ME, GH)	4	780	oxic	BM, CIC	80	–62 to –72	–48 to –52[7]	–38 to –44	–102 to –133 [0 to 22][8]
Mediterranean Seeps (ME, GH)	14	~ 2000	oxic	BM, CIC	10 to 18	—	–30 to –43[9]	–27 to –33	–62 to –111 [0 to 30][10]
Gulf of Mexico (ME, GH)	~7	540, 839	oxic	BM, CIC	80, 111[5]	–49 to –63	–28 to –34	–30 to –34	–82 to –99 [0 to 30]
Aleutian Subduction Zone (FV)	1	4800	oxic	UM, CIC	—	—	–59 to –63[11]	–39 to –42	–71 to –130 [3 to 16]
Guaymas Basin (HTV)	2 to 31[12]	2000	suboxic	BM	12 to 16[13]	-43 to –51[13]	–8 to –13[14]	–19 to –25	–58 to –89 [0 to 2.5]
Black Sea (ME)	9[15]	190, 230	anoxic	MM	30[5]	–62 to –68	–38 to –45[16]	—	–75 to –107 [0 to 2]

— indicates that information is not available.

(1) Temperatures, concentrations, and $\delta^{13}C$ values correspond to nearest sampling sites and closest sediment depth intervals that the data allow. (2) ME (methane ebullition or emissions); GH (near-surface gas hydrates); FV (fluid venting); HTV (hydrothermal venting). (3) BM (*Beggiatoa* [or other sulfide oxidizing bacteria] mats); MM (microbial mat containing sulfate-reducing bacteria and archaea); UM (microbial mat, type not specified); CIC (chemoautotrophic invertebrate communities). (4) Range of values reported for biomarkers considered to be of methanogen-archaeal origin: archaeol, hydroxyarchaeol, crocetane, and pentamethylicosane (Hinrichs and Boetius, 2002). (5) CH_4 bubbles emanating from sediment were noted; concentration is estimated from solubility in seawater at *circa in situ* temperature and pressure (Duan and others, 1992). (6) Calculated from reported $\delta^{13}C$-ΣCO_2 (−27‰), 4 °C, assumed pH = 7.5 (Zhang and others, 1995). (7) Calculated as in (6), using reported $\delta^{13}C$-ΣCO_2 (−38.8 and −41.5‰) values for the 0 to 2 cm interval at microbial mat site. (8) Relatively "heavy" values ($\delta^{13}C$ = −37 to −89‰) from off-summit sites (slope and first ridge) are not included in range. (9) Calculated as in (6), using reported $\delta^{13}C$-ΣCO_2 (−20 to −33‰) values for methane oxidation zone (10 to 20 cm). (10) Only includes methane seep sites reported in Pancost and others (2000; 2001). (11) Calculated assuming isotopic equilibrium between CO_2(aq) and authigenic carbonates (reported $\delta^{13}C$ = −45 to −49‰); $\varepsilon_{aragonite/HCO3}$ = 2‰ (Zeebe and Wolf-Gladrow, 2001). (12) Temperature range assumes linear temperature gradient in upper 2 cm of sediment. (13) Values correspond to CH_4 in hydrothermal vent fluids, and may differ from concentration/isotopic composition in surficial sediment porewater. (14) Values corresponds to CO_2(g) extracted from chimney and mound deposits, and may differ from $\delta^{13}C$-CO_2 in surface sediment porewater. (15) Estimated from temperature *versus* depth data in Weber and others 2001. (16) Calculated as in (11) using reported $\delta^{13}C$-$CaCO_3$ values (−25 to −32‰).

Sources:

Eel River Basin: Hinrichs and others (1999); Hinrichs and others (2000); Orphan and others (2001a); Orphan and others (2001b); Orphan and others (2002). Hydrate Ridge: Elvert and others (1999); Boetius and others (2000); Elvert and others (2001); Valentine and others (2005). Mediterranean Seeps: Pancost and others (2000); Pancost and others (2001); Werne and others (2002); Haese and others (2003); MEDINAUT/MEDINETH Shipboard Scientific Parties (2000). Gulf of Mexico: Zhang and others (2002); Zhang and others (2003); Roberts (2001); Sassen and others (1999). Aleutian Subduction Zone: Elvert and others (2000); Suess and others (1998). Guaymus Basin: Teske and others (2002); Peter and Shanks (1992). Black Sea: Thiel and others (2001); Michaelis and others (2002).

The link to methane oxidation rests largely on the assumption that methanotrophy is the most likely source of "ultra-light" carbon in ^{13}C-depleted archaea. As suggested by Londry and others (2008), this assumption should be examined carefully. Complex physics and sampling problems that are inherent in dynamic, methane-rich seep/vent environments make it difficult to corroborate the existence, zonation, and magnitude of net methane oxidation by checking for mass-balance and concordance among multiple indicators.

In this paper, we take a fresh look at possible sources of "ultra-light" carbon and consider autotrophic methanogenesis as well as anaerobic methanotrophy. We derive general equations based on isotope mass-balance and calibrated with field and laboratory data to show that δ^{13}C values of archaeal biomass and lipids at methane seep and vent sites are readily accounted for by isotope fractionation during methane production from CO_2. We also apply a spherical diffusion-reaction model to demonstrate that significant gradients in δ^{13}C-CO_2 within archaea/SRB aggregates are not possible.

AUTOTROPHIC METHANOGENESIS

Anabolic and catabolic pathways operating during CO_2-reduction by methanogenic archaea can be viewed as a network of reactions in which carbon flows through five reversible, non-branching reactions followed by a branch point where fixed carbon is either assimilated into biomass or dissimilated to methane (fig. 1). Rees (1973) and Hayes (1993, 2001) present excellent overviews of isotope mass-balance expressions for reaction networks comprised of reversible and irreversible reactions. Important lessons from these works are that at steady-state, the overall isotope effect for reversible, non-branching reactions depends on the degree of reversibility; for irreversible reactions, isotope effects are expressed in the material transmitted by metabolic reactions only when there is a branch point. As a result, the δ^{13}C of methane produced by CO_2 reduction, $\delta(CH_4)$, depends on the δ^{13}C of reactant, $\delta(CO_2)$, the isotope effect (ε_{ab}) and degree of reversibility (X_b) for the reduction of CO_2 to CHO—MFR (*N*-formyl-methanofuran), isotopic fractionation arising from the difference between isotope effects associated with forward and reverse flow (represented by ε'), and the carbon budget and isotope effects at the assimilation-dissimilation branch point [see Appendix, equation (A11)]:

$$\delta(CH_4) \approx \delta(CO_2) - (\varepsilon_{ab} + X_b\varepsilon') + f_h\Delta\varepsilon, \quad (1)$$

where f_h is the branching ratio (the fraction of carbon flow to the branch point that is assimilated), and $\Delta\varepsilon$ ($\equiv\varepsilon_{fh} - \varepsilon_{fg}$) is the difference between isotope effects associated with the first anabolic (ε_{fh}) and catabolic (ε_{fg}) reactions after the assimilation-dissimilation branch point. Rearranging equation (1) yields an expression for the overall isotope effect associated with methane production from CO_2 (ε_{CO_2/CH_4}):[1]

$$\varepsilon_{CO_2/CH_4} \approx (\varepsilon_{ab} + X_b\varepsilon') - f_h\Delta\varepsilon. \quad (2)$$

Acetyl—CoA (CH_3—CO—S—CoA) is the basic anabolic building block in CO_2-reducing methanogens (Simpson and Whitman, 1993). The methyl-carbon in

[1] Following Hayes (2001), we use an approximate expression for the isotope effect associated with the conversion of reactant (I) to product (J):

$$\varepsilon_{ij} \approx \delta(I) - \delta_j,$$

where $\delta(I)$ is the δ^{13}C-value of reactant I and δ_j denotes the isotopic composition of carbon being transmitted by the reaction $I \rightarrow J$. Errors introduced by this approximation are small (Zeebe and Wolf-Gradrow, 2001) and should not affect the overall conclusions.

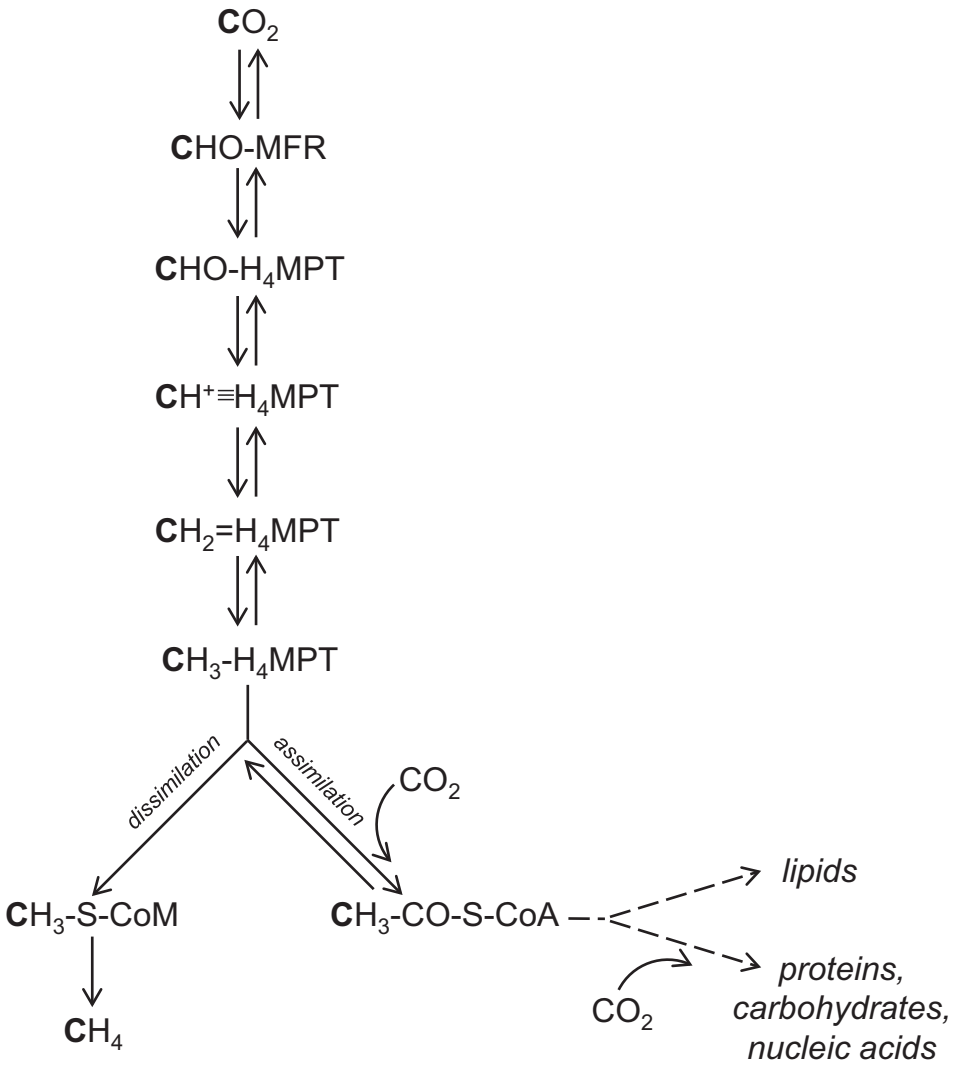

Fig. 1. Catabolic and anabolic pathways for autotrophic methanogenesis (after Simpson and Whitman, 1993). Two-way arrows represent reversible reactions, dashed arrows indicate multiple reaction steps, and the boldface **C** represents the carbon fixed into CHO-MFR. Abbreviations: CHO—MFR (*N*-formyl-methanofuran), CHO—H_4MPT (N^5-formyl-tetrahydromethanopterin), $CH^+{\equiv}H_4$MPT (N^5,N^{10}-methenyl-tetrahydromethanopterin), $CH_2{=}H_4$MPT (N^5,N^{10}-methylene-tetrahydromethopterin), CH_3—H_4MPT (N^5-methyl-tetrahydromethopterin), CH_3—S—CoM (methyl-coenzyme M), CH_3—CO—S—CoA (acetyl-coenzyme A).

acetyl—CoA comes from the methyl-group in CH_3—H_4MPT (N^5-methyl-tetrahydromethopterin) (fig. 1), and the $\delta^{13}C$ of biomass derived from this methyl-carbon (δ_h) is fixed by mass balance in accord with equation (A12) (see Appendix):

$$\delta_h \approx \delta(CO_2) - (\varepsilon_{ab} + X_f\varepsilon') - (1 - f_h)\Delta\varepsilon. \quad (3)$$

In contrast, the carbonyl moiety in acetyl—CoA is obtained by reduction of intracellular CO_2 (Simpson and Whitman, 1993; fig. 1). Combining equations (2) and (3) yields:

$$\delta_h \approx \delta(CO_2) - \varepsilon_{CO_2/CH_4} - \Delta\varepsilon. \quad (4)$$

Although acetyl—CoA is the main source of carbon for lipid biosynthesis in autotrophic methanogens, other cellular components such as proteins require additional CO_2-fixing steps (Hayes, 2001). Lacking detailed information regarding isotope effects and branching ratios associated with the portion of biomass not derived from the methyl-carbon in acetyl—CoA, we aggregate these unknown elements into a single term in the isotope mass-balance equation for cell carbon:

$$\delta(B) = f_M\delta_h + (1 - f_M)(\delta(CO_2) - \bar{\varepsilon}), \quad (5)$$

where $\delta(B)$ is the $\delta^{13}C$ of methanogen biomass, f_M is the fraction of cell carbon derived from the methyl-group of acetyl—CoA, and $\bar{\varepsilon}$ is the weighted average isotope effect for all other carbon fixing reactions. Combining equations (4) and (5):

$$\delta(B) \approx f_M(\delta(CO_2) - \varepsilon_{CO_2/CH_4} - \Delta\varepsilon) + (1 - f_M)(\delta(CO_2) - \bar{\varepsilon}). \quad (6)$$

Rearranging and setting $\varepsilon_{CO_2/B} \approx \delta(CO_2) - \delta(B)$ yields:

$$\varepsilon_{CO_2/B} \approx f_M\varepsilon_{CO_2/CH_4} + f_M\Delta\varepsilon + (1 - f_M)\bar{\varepsilon}. \quad (7)$$

Equation (7) predicts that $\varepsilon_{CO_2/B}$ scales with ε_{CO_2/CH_4}, and that the relationship between $\varepsilon_{CO_2/B}$ and ε_{CO_2/CH_4} is independent of the degree of reversibility of the first five reactions in the CO_2 reduction pathway. The undetermined coefficients (f_M, $\Delta\varepsilon$, and $\bar{\varepsilon}$) can be constrained using paired ε_{CO_2/CH_4} and $\varepsilon_{CO_2/B}$ data from laboratory studies, provided that intra- and extracellular CO_2 and methane have similar isotope ratios. This is likely to be the case. Isotopic fractionation during diffusive transport of dissolved CO_2 and methane across the cell membrane is small (for example, O'Leary, 1984). Furthermore, intracellular gradients in $\delta^{13}C$-CO_2 and $\delta^{13}C$-CH_4 are minimal owing to the relatively long residence times for intracellular CO_2 and methane compared to the time scale for diffusive mixing over the distance of a microbial cell (see $\delta^{13}C$-CO_2 MICRO-GRADIENTS, below).

Eight studies using a variety of autotrophic methanogen cultures have measured the isotopic discrimination between the substrate, CO_2, and the resulting methane and biomass (table 2). These studies were conducted at elevated temperatures (34 to 100 °C) compared to most methane seep and vent sites (table 1) and used widely varying experimental conditions. We used the regression line for $\varepsilon_{CO_2/B}$ versus ε_{CO_2/CH_4} (fig. 2) to calibrate the coefficients in equation (7): $f_M = 0.73 \pm 0.07$ and $f_M\Delta\varepsilon + (1 - f_M)\bar{\varepsilon} = -1.6 \pm 2.5$ (uncertainties in slope and intercept denote standard errors). Substituting $\varepsilon_{CO_2/B} \approx \delta(CO_2) - \delta(B)$ and regression coefficients into equation (7), we arrive at an expression for predicting the $\delta^{13}C$ of biomass resulting from autotrophic methanogenesis:

$$\delta(B) \approx \delta(CO_2) - (0.73\varepsilon_{CO_2/CH_4} - 1.6). \quad (8)$$

Botz and others (1996) used a flow-through fermentation system to measure ε_{CO_2/CH_4} for pure cultures of CO_2-reducing, methanogenic archaea grown at 35 to 85 °C. They found that carbon isotopic fractionation for cells that are in stationary growth phase (which they argue "is the status of methanogens in most natural marine sediments", p. 262) is similar to that of autotrophic methanogens in natural sediments at comparable temperatures.[2] Furthermore, they combined their results with a large

[2] Botz and others (1996) observed that ε_{CO_2/CH_4} values from cultures in log-phase growth tend to be much lower than those from the same organisms during stationary growth. Valentine and others (2004) provide a convincing explanation for this observation: ε_{CO_2/CH_4} values scale with overall reversibility of CO_2 reduction (X_b) [see eq (2)], and X_b is inversely related to energy yield and growth rate. Subsequent work (Penning and others, 2005) has confirmed this explanation.

TABLE 2

Paired ε_{CO_2/CH_4} and $\varepsilon_{CO_2/B}$ values for pure cultures of CO_2-reducing methanogens[1]

Organism	Temp (°C)	ε_{CO_2/CH_4} (‰)	$\varepsilon_{CO_2/B}$ (‰)	Experimental Conditions[2]	Reference[3]
Methanosarcina barkeri	40	44.9	14.8	O, L, 80	A*
Methanobacterium strain M.o.H.	40	44.8	11.5	O, L, 80	A*
Methanobacterium strain M.o.H.	40	61.5	-7.5	O, L, 80	A[4]
Methanobacterium thermoautotrophicum	65	30.1	12.7	C, V, 80	A[5]
Methanobacterium thermoautotrophicum	65	39.7	26.6	C, V, 80	A[6]
Methanobacterium thermoautotrophicum	65	62.7	43.8	C, V, 80	A[7]
Methanobacterium thermoautotrophicum	65	63.5	46.0	C, V, 80	A[7]
Methanobacterium thermoautotrophicum	65	35.2	24.5	O, –, 80	B[8]
Methanobacterium thermoautotrophicum	65	39.5	21.9	O, –,80	B[9]
Methanobacterium thermoautotrophicum	65	35.4	23.1	O, –,80	B[10]
Methanobacterium sp. strain ivanov	37	36.5	25.2	O, –,80	C
Methanobacterium sp. strain ivanov	37	34.9	23.2	O, –,80	C
Methanobacterium sp. strain ivanov	46	33.4	18.5	O, –,80	C
Methanobacterium sp. strain ivanov	46	35.5	24.3	O, –,80	C
Methanobacterium thermoautotrophicum	56	38.7	27.0	O, –,80	D
Methanobacterium thermoautotrophicum	56	29.0	26.6	O, –,80	D
Methanobacterium thermoautotrophicum	66	44.1	27.4	O, –,80	D
Methanobacterium formicium	34	49.5	36.1	C, –,80	E
Methanobacterium formicium	34	50.8	38.4	C, –,80	E
Methanobacterium formicium	34	46.6	34.7	C, –,80	E
Methanobacterium thermoautotrophicum	–	41.0	34.0	–, –, –	F
Methanobacterium thermoautotrophicum	65	24.6	15.0	C, E, 80	G
Methanococcus igneous	85	28.4	20.2	C, E, 80	G

Table 2
(continued)

Organism	Temp (°C)	ε_{CO_2/CH_4} (‰)	$\varepsilon_{CO_2/B}$ (‰)	Experimental Conditions[2]	Reference[3]
Methanococcus jannaschii	85	25.0	6.2	C, E, 80	G
Methanococcus thermolithotrophicus	65	29.0	22.7	C, E, 80	G
Methanococcus thermolithotrophicus	65	29.6	25.8	C, E, 80	G
Methanococcus thermolithotrophicus	65	29.5	26.7	C, E, 80	G
Methanococcus thermolithotrophicus	41	26.2	7.4	C, E, 80	G
Methanococcus thermolithotrophicus	51	27.0	13.5	C, E, 80	G
Methanococcus thermolithotrophicus	60	26.4	19.7	C, E, 80	G
Methanococcus thermolithotrophicus	65	29.8	24.8	C, E, 80	G
Methanococcus thermolithotrophicus	65	30.8	26.0	C, E, 80	G
Methanococcus thermolithotrophicus	70	27.9	24.9	C, E, 80	G
Methanopyrus kandleri	100	30.0	20.3	C, E, 80	G
Methanopyrus kandleri	100	27.6	12.7	C, E, 80	G
Methanosarcina barkeri	37	17.2	19.5	C, E, 80	G
Methanothermus fervidas	85	30.6	13.1	C, E, 80	G
Methanococcus jannaschii	85	17.7	17.7	C, E, 80	G
Methanococcus jannaschii	85	19.6	10.7	C, E, 80	G
Methanococcus jannaschii	85	19.6	13.7	C, E, 80	G
Methanococcus thermolithotrophicus	65	24.9	8.7	C, E, 80	G
Methanococcus thermolithotrophicus	45	21.1	20.5	C, E, 80	G
Methanococcus thermolithotrophicus	45	23.0	13.4	C, E, 80	G
Methanococcus thermolithotrophicus	45	16.5	4.8	C, E, 80	G
Methanococcus thermolithotrophicus	65	23.2	22.0	C, E, 80	G
Methanosarcina barkeri	37	43.4	14.6	C, –, 80	H[11]*
Methanosarcina barkeri	37	55.5	16.3	C, –, 5	H[11]*

— indicates that information is not available.

(1) ε_{CO_2/CH_4} and $\varepsilon_{CO_2/B}$ were not reported in references A, B, C, D, E, F, and H; hence, we calculated ε-values as follows. For open system experiments, gassing rates are high, CO_2 can be treated as an infinite reservoir, and isotope effects are calculated as:

$$\varepsilon_{CO_2/CH_4} = [\delta(CO_2) - \delta(CH_4)]/[1 + (\delta(CH_4)/1000)] \text{ and}$$
$$\varepsilon_{CO_2/B} = [(\delta(CO_2) - \delta(B)]/[1 + \delta(B)/1000)],$$

where $\delta(CO_2)$ and $\delta(CH_4)$ are $\delta^{13}C$ values of output gases (Games and others, 1978). For closed system experiments, isotope effects are estimated as:

$$\varepsilon_{CO_2/CH_4} \approx \delta(CO_2) - \delta(CH_4) \text{ and } \varepsilon_{CO_2/B} \approx \delta(CO_2) - \delta(B).$$

(2) Incubation system (Open [O] or Closed [C]); growth phase of microorganisms (early log phase [E, < 10% of CO_2 consumed], log phase [L], or variable [V]); H_2 partial pressure (80% [80] or 5% [5]). For closed-system experiments in which growth continued into the mid- or late-stages of the log phase, reported ε-values may not reflect true isotope effects due to closed-system effects. (3) A: Games and Hayes (1976). B: Fuchs and others (1979). C: Belyaev and others (1983). D: Baresi and others (1983). E: Balabane and others (1987). F: Takigiku (1987); reported in Summons and others (1998). G: House and others (2003). H: Londry and others (2008). (4) This result, in which the methanogen biomass was enriched in ^{13}C relative to CO_2, is not included in figure 2. Games and Hayes (1976) note that: "It seems inconceivable that this effect could occur if the metabolism of the cell involved conversion of CO_2 to cell mass and methane, but further experiments to substantiate this anomalous effect have not been conducted" (p. 57). (5) ε-values were calculated for 5.5 hr incubation time. (6) ε-values were calculated for 13 hr incubation time. (7) ε-values were calculated for 48 hr incubation time. (8) $\delta^{13}C$-values used to calculate isotope effects have been extrapolated to infinite gassing rate. (9) Gassing rate: 10 mL/min. (10) Gassing rate: 300 mL/min. (11) $\delta(CH_4)$-values refer to methane at the end of the experiment. * Data are considered to be outliers (open circles in figure 2) and are not included in the regression.

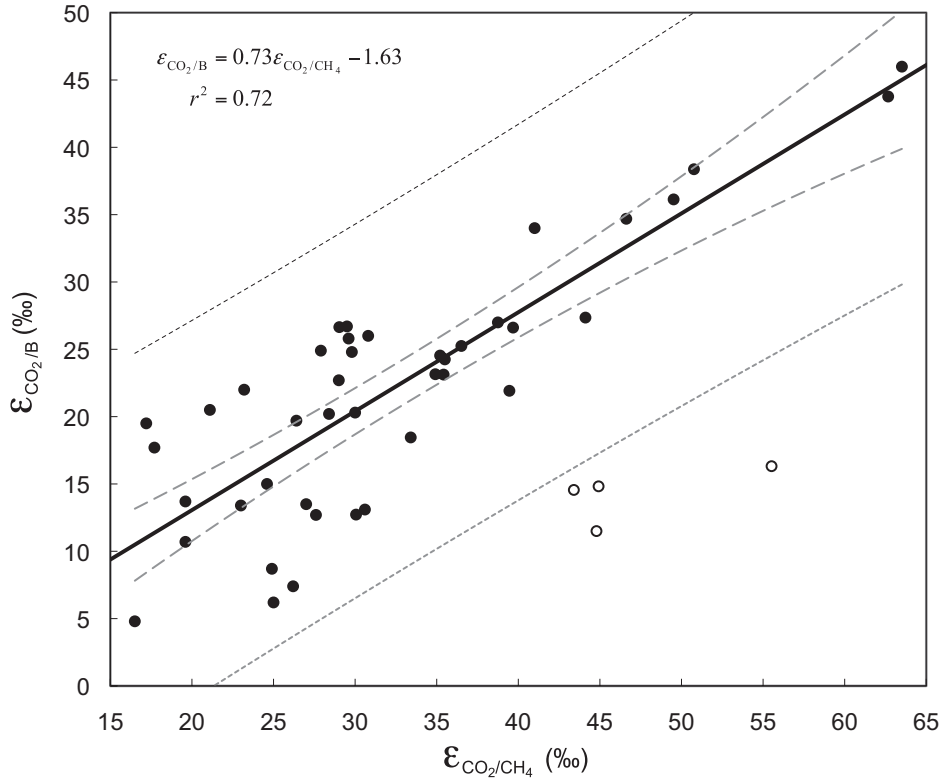

Fig. 2. $\varepsilon_{CO_2/B}$ versus ε_{CO_2/CH_4} for autotrophic methanogenic archaea (table 2). The solid line is the least-squares linear regression; the best-fit equation and coefficient of determination are printed in the upper left-hand corner. The long-dashed lines are the 95% confidence interval of the regression line; the probability is 95% that these two curved bands enclose the true best-fit linear regression line. The short-dashed lines define the area in which we expect 99% of the data points to fall; the four points outside this region (open circles) are taken to be outliers and were not included in the regression.

database of fractionation factors based on paired $\delta^{13}C$-CO_2 and $\delta^{13}C$-CH_4 values from marine sediments (−1 to 58 °C; Whiticar and others, 1986) and found that isotopic fractionation during microbial methane-production closely approaches that predicted by isotopic equilibrium:

$$10^3 \ln \alpha = 29.2 \left(\frac{10^3}{T}\right) - 29.6, \quad (9)$$

where α is the equilibrium fractionation factor for CO_2-CH_4 isotopic exchange and T is absolute temperature.[3] Although there is no fundamental reason why kinetic and equilibrium isotope effects should be the same, equation (9) provides a convenient means of calculating the isotope effect for autotrophic methanogenesis ($\varepsilon_{CO_2/CH_4} \equiv (\alpha - 1)10^3$), and appears to be representative over a wide range of temperature (−1 to 85 °C).

[3] Equation (9) is from Whiticar and others (1986), and is based on equilibrium fraction factors calculated by Richet and others (1977).

If methanogenic archaea utilize the CO_2-reduction pathway at methane seep and hydrothermal vent sites, the isotopic composition of the resulting biomass is readily predicted from equations (8) and (9). At Eel River Basin, $\delta(CO_2)$ (equal to $\delta^{13}C$ of bulk porewater CO_2; see $\delta^{13}C$-CO_2 MICRO-GRADIENTS, below) is −38 permil [calculated from the reported $\delta^{13}C$-ΣCO_2 (−27‰; Orphan and others, 2002) and *in situ* temperature (4 °C; Orphan and others, 2001b), and assumed pH (7.5; Zeebe and Wolf-Gladrow, 2001; Zhang and others, 1995) and ε_{CO_2/CH_4} at 4 °C is 79‰ (eq (9))]. The predicted δ(B) value (−94‰) compares well with the "lightest" value reported for archaeal cells in the interior of archaea/SRB aggregates (−96‰; Orphan and others, 2001b).

A similar approach is used to calculate the $\delta^{13}C$ of lipid biomarkers, δ(L), derived from autotrophic methanogens:

$$\delta(L) \approx \delta(B) - \varepsilon_{B/L}, \tag{10}$$

where positive values for $\varepsilon_{B/L}$ reflect the observation that "lipids are light" (Hayes, 1993). Combining equations (8) and (10),

$$\delta(L) \approx \delta(CO_2) - (0.73\varepsilon_{CO_2/CH_4} - 1.6) - \varepsilon_{B/L}. \tag{11}$$

Only two studies to date report the magnitude of ^{13}C-depletion in lipids relative to biomass in CO_2-reducing methanogens. Takigiku (ms, 1987)[4] found that lipids are 13 permil "lighter" than biomass in *Methanobacterium thermoautotrophicum*. Londry and others (2008) found that pentamethylicosane, archaeol, and *sn*-2 hydroxyarchaeol are not significantly "lighter" than biomass in *Methanosarcina barkeri* supplied with abundant H_2 (average $\varepsilon_{B/L}$ = 1.2 ± 4.1‰); however, these lipids are 29.7 ± 1.9 permil "lighter" than biomass when the same organisms were cultured with limited H_2.[5] Given the sparse and disparate $\varepsilon_{B/L}$ data, we adopt an average value of 14 permil.

If CO_2-reducing methanogens are active at methane seep and hydrothermal vent sites, the isotopic composition of their lipids can be calculated from *in situ* $\delta(CO_2)$ and temperature according to equations (9) and (11). However, $\delta^{13}C$ values of porewater CO_2 are not available for some of these sites, and must be calculated from $\delta^{13}C$-ΣCO_2 (assuming CO_2—HCO_3^-—CO_3^{2-} isotopic equilibrium) or from the $\delta^{13}C$ of authigenic carbonates (assuming that authigenic aragonite precipitates in isotopic equilibrium with porewater ΣCO_2). Furthermore, the available isotopic data for inorganic carbon do not always correspond to the exact location and sediment depth interval as the samples analyzed for archaeal lipids. The values summarized in table 1 represent our best estimate of pertinent $\delta(CO_2)$ values; details for each estimate are provided in footnotes to the table.

In figure 3, we compare predicted $\delta^{13}C$ values for lipids derived from CO_2-reducing methanogens with measured $\delta^{13}C$ values for archaeal lipids in methane seep and hydrothermal vent sediments. Predicted values clearly fall within the realm of "ultra-light" carbon and within the range of measured values. Since lipids produced by acetoclastic methanogenesis are "heavier" than those produced by autotrophic methanogenesis (Londry and others, 2008), variable amounts of acetate fermentation concurrent with CO_2 reduction could explain the large range of observed $\delta^{13}C$ values and why predicted values are generally at the low end of the observed ranges.

These results are not meant to provide evidence of autotrophic methanogenesis at methane seep and vent sites [see our companion paper (Alperin and Hoehler, 2009) for a discussion of thermodynamic and physical constraints on anaerobic methane

[4] Reported in Hayes (2001); the individual lipids are not specified but are indicated to be isoprenoidal.
[5] Londry and others (2008) point out that their reported isotopic discriminations may not be true fractionation factors due to insufficient data to correct for closed-system effects.

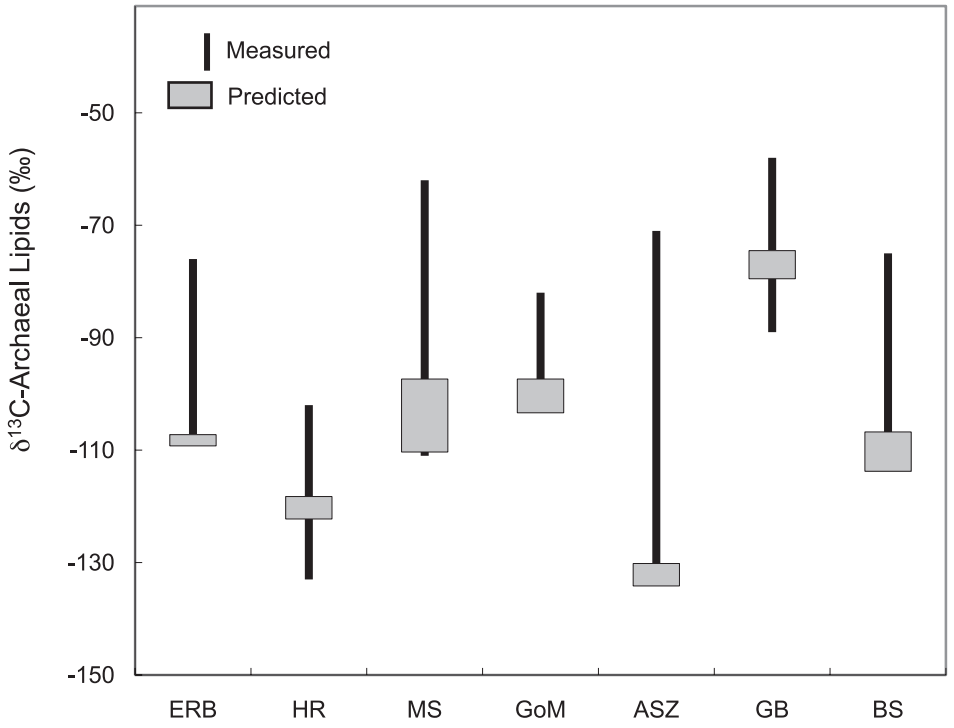

Fig. 3. Measured and predicted $\delta^{13}C$ values of archaeal lipids in sediments from methane seep and hydrothermal vent sites. The vertical lines mark the range of measured values for archaeol, hydroxyarchaeol, crocetane, and pentamethylicosane (table 1). The gray rectangles denote $\delta^{13}C$ values for lipids derived from autotrophic methanogenesis predicted from equations (9) and (11) for environmental conditions in table 1 [for Guaymas Basin sediments, the average temperature in the 0 to 2.5 cm interval (17° C) was used]. The height of the rectangles reflects variability in $\delta^{13}C$-CO_2. Published interpretations of archaeal lipids with $\delta^{13}C$ values $< -60‰$ have tended to focus on methanotrophic rather than methanogenic sources. Abbreviations: ERB (Eel River Basin), HR (Hydrate Ridge), MS (Mediterranean Seeps), GoM (Gulf of Mexico), ASZ (Aleutian Subduction Zone), GB (Guaymus Basin), BS (Black Sea).

oxidation in archaea/SRB aggregates]. Rather, they illustrate that it is conceivable that "ultra-light" biomass and lipids in seep/vent sediments are derived from CO_2-reducing methanogenic archaea.[6] The inference of anaerobic methanotrophy based on ^{13}C depletion in archaeal cell carbon and/or lipids should thus be considered tentative unless corroborated by independent, concordant evidence of net methane consumption; for example, upward concavity in the methane profile combined with depth distributions of $\delta^{13}C$-CH_4 and methane-oxidation rates, or *in vitro* experiments that are both well-controlled (to correct for any decrease in methane concentration that is not due to microbial oxidation) and over-determined (to assure internal consistency).

ANAEROBIC METHANOTROPHY

A plausible outline of anabolic-catabolic pathways operating during anaerobic methane oxidation is shown in figure 4. The outline is necessarily sparse, as the mechanism and organisms(s) are still a matter of debate. Nevertheless, we can

[6] Autotrophic methanogenesis will not always result in "ultra-light" lipids since porewater ΣCO_2 in methanogenic sediments can be highly enriched in ^{13}C. For example, $\delta^{13}C$-ΣCO_2 approaches $+20‰$ in methanogenic sediments from Eckernförde Bay (Martens and others, 1999).

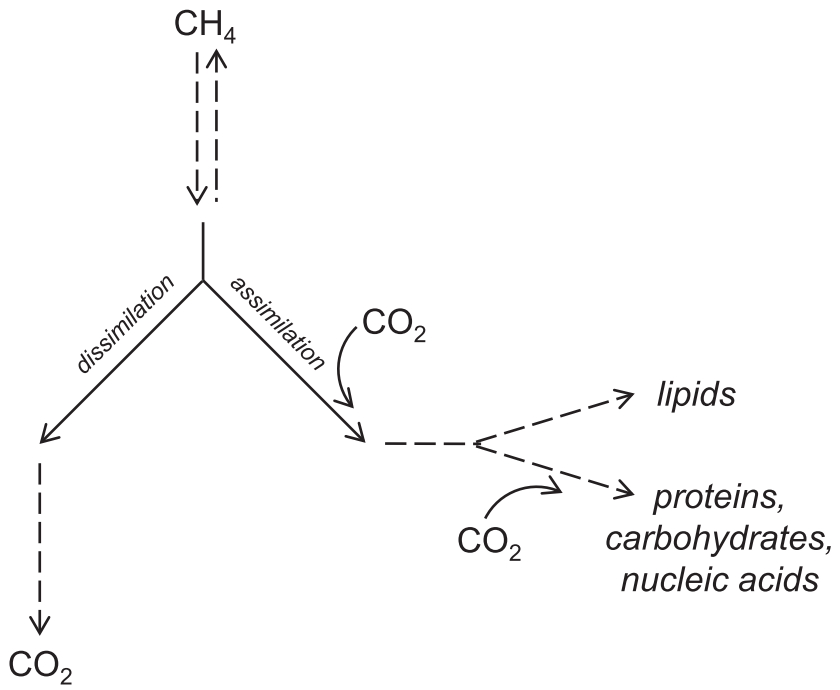

Fig. 4. Outline of possible catabolic and anabolic reactions during anaerobic methane oxidation. Two-way arrows represent reversible reactions, and dashed arrows indicate the possibility of multiple reaction steps.

constrain the isotopic fractionation between methane and biomass by making several assumptions:

a) Activated methane flows through one or more reversible reactions followed by a branch point where the intermediate compound containing the fixed methane is either assimilated into biomass or dissimilated to CO_2.
b) Isotopic fractionation due to reverse carbon flow is minimal after the assimilatory-dissimilatory branch point.
c) Intracellular CO_2 may be fixed after the biosynthetic branch point to create the carbon backbones necessary to synthesize cellular components.

With these assumptions, the reaction network for anaerobic methanotrophy parallels that for autotrophic methanogenesis (compare figs. 1 and 4). Hence, the isotope mass-balance equation for cell carbon in anaerobic methane-oxidizing organisms is analogous to equation (6):

$$\delta(\mathrm{B}) \approx f_{\mathrm{M}}(\delta(\mathrm{CH_4}) - \varepsilon_{\mathrm{CH_4/CO_2}} - \Delta\varepsilon) + (1 - f_{\mathrm{M}})(\delta(\mathrm{CO_2}) - \bar{\varepsilon}), \qquad (12)$$

where $\delta(\mathrm{B})$, $\delta(\mathrm{CH_4})$, and $\delta(\mathrm{CO_2})$ are the $\delta^{13}\mathrm{C}$ values of methanotrophic biomass, reactant methane, and intracellular CO_2, respectively, f_{M} is the fraction of cell carbon derived from methane, $\varepsilon_{\mathrm{CH_4/CO_2}}$ is the kinetic isotope effect during AMO, $\Delta\varepsilon$ ($\equiv \varepsilon_{\mathrm{AN}} - \varepsilon_{\mathrm{CAT}}$) is the difference between isotope effects associated with the first anabolic ($\varepsilon_{\mathrm{AN}}$) and catabolic ($\varepsilon_{\mathrm{CAT}}$) reactions after the assimilation-dissimilation branch point, and $\bar{\varepsilon}$ is the weighted average isotope effect for non-methane carbon fixation sites.

Table 3

Kinetic isotope effects for anaerobic methane oxidation

Study site	Temperature (ºC)	ε_{CO_2/CH_4} (‰)	Method
Sediment studies			
Compilation[1]	—	4.0	Rayleigh model
Marsh environments[1]	—	8.5	C_2 + model[8]
Brackish environments[1]	—	7.9	C_2 + model[8]
Gulf of Mexico[1]	—	7.1	C_2 + model[8]
Mississippi River Delta[1]	—	14.3	C_2 + model[8]
Antarctica[1]	—	1.8 to 4.9	C_2 + model[8]
Skan Bay, AK[2]	4	8.8 ± 1.3	Diagenetic model
Eckernforde Bay, FRG[3]	8	12 ± 1	Diagenetic model
Norman Landfill, OK[4]	—	14 ± 1	Rayleigh model
White Oak River estuary, NC[5]	28	17	Diagenetic model
Water column studies			
Black Sea[6]	8.9	21 ± 1	Open-system model
Enrichment cultures			
Hydrate Ridge[7]	12	12 ± 0	Rayleigh model
Amon Mud Volcano[7]	20	21 ± 3	Rayleigh model
Black Sea (microbial mat)[7]	12	37 ± 3	Rayleigh model
Average		13 ± 9	

— indicates that information is not available.
[1] Whiticar and Faber (1986). [2] Alperin and others (1988). [3] Martens and others (1999). [4] Grossman and others (2002). [5] K.G. Lloyd, Center for Geomicrobiology, Aarhus, Denmark, submitted. [6] Kessler and others (2006). [7] Holler and others (2009). [8] ε_{CO_2/CH_4} is calculated from $C_1/(C_2 + C_3)$ versus $\delta^{13}C\text{-}CH_4$, where C_1 is methane, C_2 is ethane, and C_3 is propane concentration (see Whiticar and Faber, 1986).

Assuming that maximum ^{13}C depletion in methanotrophic biomass occurs when methane is the dominant source of cell carbon (that is, $f_M \approx 1$), the lower limit for $\delta(B)$ is:

$$\delta(B) \geq \delta(CH_4) - \varepsilon_{CH_4/CO_2} - \Delta\varepsilon. \quad (13)$$

Since inverse kinetic isotope effects for carbon are unknown (Hayes, 1993), ε_{CAT} must be ≥ 0. Thus, the minimum value for ε_{AN} occurs when $\varepsilon_{CAT} = 0$:

$$\varepsilon_{AN} \geq \delta(CH_4) - \delta(B) - \varepsilon_{CO_2/CH_4}. \quad (14)$$

Equation (14) provides a lower-limit constraint on the magnitude of the isotope effect associated with the anabolic arm of the assimilatory-dissimilatory branch point during anaerobic methane oxidation.

The overall isotope effect during AMO (ε_{CH_4/CO_2}) has never been measured for pure cultures, but a number of studies provide estimates based on ^{13}C enrichment in residual (unoxidized) methane in anoxic sediments, water column, and *in vitro* enrichment cultures (table 3). These estimates come from a variety of marine and brackish environments where the relevant methane concentrations range from < 0.1 to > 3 mM and probably encompass both methane-limited and non-limited conditions. The estimated values for ε_{CH_4/CO_2} average 13 ± 9 permil, and indicate that overall isotopic selectivity in anaerobic methanotrophs is much less than in autotrophic

methanogens [compare $\varepsilon_{CO_2/CH_4} = 77‰$ at 8 °C (eq (9))]. A smaller isotope effect for methanotrophy is expected due to the greater bond enthalpy in CO_2 relative to methane.[7] When the force binding the nuclei is strong, the electronic potential energy well is said to be "tight", and the isotopic difference in zero-point vibrational energy is large (Huskey, 1991). Thus, a stronger bond to the isotopic atom in the reactant translates to a larger kinetic isotope effect (O'Leary, 1980).

If anaerobic methanotrophs are a source of "ultra-light" biomass in methane-seep sediments, the lower-limit value for ε_{AN} is readily constrained from equation (14). At Eel River Basin, $\delta(CH_4)$ averages −50 permil and δ(B) reaches −96 permil (Orphan and others, 2001b). Given $\varepsilon_{CH_4/CO_2} \approx 13‰$ (table 3), ε_{AN} would have to be at least 33 permil in order for methane to serve as carbon source. Enzymatic isotope effects of this magnitude are common (that is, $\varepsilon = 30‰$ for CO_2 fixation by Rubisco; $\varepsilon = 52‰$ for CO_2 fixation by carbon monoxide dehydrogenase; $\varepsilon = 34‰$ for decarboxylation of L-malate by malic enzyme; Hayes, 2001; Weiss, 1991), but generally correspond to the initial fixation of inorganic carbon or decarboxylation reactions. We are not aware of isotope effects this large for reactions in which carbon is transferred among metabolic intermediates.

However, if ε_{AN} is significantly less than 33 permil and/or the limits implicit in equation (14) are not realized, biomass resulting from anaerobic methanotrophy could be *less* ^{13}C-depleted than biomass derived from autotrophic methanogenesis. This possibility is difficult to test empirically for methane seep and vent sediments that contain "ultra-light" archaeal carbon because net methane reaction rates (production minus oxidation) are not known. However, one study conducted in Kattegat Strait, a typical non-seep marine sediment, reports "ultra-light" isotopic values ($\delta^{13}C < -60‰$) for crocetane (an isoprenoid lipid of presumed archaeal origin; Bian and others, 2001). At this site, net methane oxidation is readily identified by the classic upward concavity in the methane profile, and a narrow subsurface peak in ^{14}C-methane-oxidation rate establishes the location of the methane-oxidation zone. Furthermore, the upward diffusive methane flux and the integrated methane-oxidation rate approach mass-balance, indicating that the concentration and rate data are concordant.[8]

Bian and others (2001) report that crocetane is absent from Kattegat sediments above the sulfate-methane transition zone. It is first detected at a depth of 185 cm—just below the well-defined peak in methane-oxidation rate (175 to 185 cm)—with a $\delta^{13}C$ value of -67.0 ± 4.7 permil. This value is not significantly different from that of sedimentary methane at a nearby site ($-72.3 \pm 0.7‰$; Bian and others, 2001). From equation (13), $\delta(B) \approx \delta(CH_4)$ suggests that $\varepsilon_{CAT} - \varepsilon_{AN} \leq 13$ permil for anaerobic methane oxidizers and/or intracellular CO_2 contributes relatively heavy carbon to methanotrophic biomass (that is, $f_M < 1$).

[7] The overall isotope effect for aerobic methanotrophs ($17 \pm 6‰$) is also much less than for autotrophic methanogens. This value is the average of the 13 studies compiled in Reeburgh (2003; his table 3) after correcting several typographical errors: the entry for Coleman and others (1981) should read "1.013–1.025" instead of "1.013–1.015"; the entry for Barker and Fritz (1981) should read "1.005–1.031" instead of "1.005–1.103"; the entries for Snover and Quay (2000) should read "1.0173 ± 0.0010" instead of "1.107 ± 0.0010" and "1.0181 ± 0.0004" instead of "1.081 ± 0.0004".

[8] The integrated methane oxidation rate is reported as 1.8 mmol m^{-2} d^{-1} (Bian and others, 2001). The diffusive flux of methane into the oxidation zone is not reported, but can be estimated from Fick's First Law (Berner, 1980). The methane concentration at 195 cm is 1.3 mM. Reliable methane concentration data from greater depth are not available; however, Laier and others (1996) observed a gas phase just below 200 cm in acoustic profiles at a nearby site, and estimate *in situ* methane saturation at 9 mM. The molecular diffusion coefficient for methane at 35 psu salinity, 5 °C is 9.1×10^{-6} cm^2 s^{-1} [Sahores and Witherspoon (1970), corrected to *in situ* temperature, salinity, and pressure after Lerman (1979)]. Given a porosity of 0.6 (Iversen and Jørgensen, 1985) and correcting for tortuosity via Ullman and Aller (1982) yields an upward diffusive methane flux of ~2.6 mmol m^{-2} d^{-1}. This value is in reasonable agreement with the integrated rate given the uncertainty in the methane concentration gradient.

The $\delta^{13}C$ of crocetane shifts abruptly ($-90.3 \pm 5.5‰$) at 190 cm, the lower boundary of the sulfate-reduction zone where sulfate concentrations appear to stabilize at < 0.5 mM. A shift in $\delta^{13}C$ of -23 permil over a 5-cm depth interval cannot be diagenetic, and indicates that the crocetane produced in the sediment horizon with peak methane-oxidation rates ($\delta^{13}C \approx -67‰$) is diluted during burial with crocetane that is far more depleted in ^{13}C ($\delta^{13}C < -90‰$). Autotrophic methanogens are a possible source of highly ^{13}C-depleted crocetane (see above), and the process may be active just below the sulfate-methane transition zone. In typical marine sediments, methane production from CO_2 commences immediately after sulfate depletion (Alperin and others, 1992; Hoehler and others, 1994) provided that the pool of reactive organic matter has not been exhausted. Furthermore, the sulfate-methane transition zone generally corresponds to a minimum in $\delta^{13}C$-ΣCO_2 (Reeburgh, 1980). Bian and others (2001) show that the small change in POC concentration (~0.05%) between 190 and 245 cm can account for only 20 percent of the upward methane flux, and suggest that most methane production occurs at greater depth. Nevertheless, some amount of CO_2 reduction above 245 cm is likely.

Thus, the one study where the occurrence of "ultra-light" archaeal lipids can be interpreted in the context of biogeochemical zonation suggests that there is an abrupt change in the process that produces crocetane at the base of the sulfate-reduction zone. Crocetane that first appears in the sediment at a depth that is nearly coincident with the peak in methane-oxidation rate is considerably less depleted in ^{13}C than crocetane produced at or below the sulfate-depletion depth where methanogenesis is generally considered to be the dominant terminal metabolic pathway.

$\delta^{13}C$-CO_2 micro-gradients

Several papers have suggested that sulfate-reducing bacteria in a tightly-packed archaea/SRB aggregate could be exposed to methane-derived CO_2 that is depleted in ^{13}C relative to the porewater CO_2 pool (Boetius and others, 2000; Werne and others, 2002). Hinrichs and Boetius (2002) use an unspecified diffusion model to argue that micro-gradients in $\delta^{13}C$-CO_2 are possible if the distance between methane-oxidizing archaea and sulfate-reducing bacteria is less than 10 μm. A simple scaling argument shows that this is not correct.[9] Here we apply an isotope diffusion-reaction model to demonstrate that significant micro-gradients in $\delta^{13}C$-CO_2 within an archaea/SRB aggregate are not possible.

Steady-state distributions of ^{12}C- and ^{13}C-CO_2 within a spherical, methanotrophic aggregate and in the surrounding porewater are given by the following equations (Crank, 1975):

$$D'\left(\frac{d^2[^{12}CO_2]}{dr^2} + \frac{2}{r}\frac{d[^{12}CO_2]}{dr}\right) + {}^{12}R = 0 \qquad (15)$$

$$D'\left(\frac{d^2[^{13}CO_2]}{dr^2} + \frac{2}{r}\frac{d[^{13}CO_2]}{dr}\right) + {}^{13}R = 0 \qquad (16)$$

where D' is the molecular diffusion coefficient for CO_2(aq) (corrected for porosity and/or tortuosity), r is radial distance from the aggregate center, ^{12}R and ^{13}R are rates

[9] The Damkohler number—$Da = k\ell^2 D^{-1}$ (where k is the fractional turnover rate of chemical i, ℓ is the length-scale of interest, and D is the diffusion coefficient)—scales the relative importance of reaction to diffusive transport (Boudreau, 1997). When $Da \ll 1$, diffusive-mixing dominates over reaction, and concentration gradients for i are minimal over distance ℓ. For $[CO_2(aq)] = 690$ μM, and a CO_2 production rate in the archaeal portion of the aggregate of 44 μM s^{-1} (table 4), $k = 44$ μM $s^{-1}/690$ μM $= 0.064$ s^{-1}. Hence, for a length-scale characteristic of an archaea/SRB aggregate ($\ell = 3.2 \times 10^{-4}$ cm) and $D_{CO_2} = 4.6 \times 10^{-6}$ cm^2 s^{-1} (table 4), $Da \sim 10^{-3} \ll 1$.

of $^{12}CO_2$ and $^{13}CO_2$ production by methane-oxidizing archaea, respectively, and the brackets denote concentration. Equations (15) and (16) neglect the slight difference in diffusion coefficients for $^{12}CO_2$(aq) and $^{13}CO_2$(aq),[10] and assume that D' is constant throughout the model domain.[11] ^{12}R and ^{13}R are calculated from the total methane oxidation rate (R) as follows:

$$^{12}R = R\frac{10^3}{(\delta_{CO_2} + 10^3)\Re_{V\text{-}PDB} + 10^3} \tag{17}$$

$$^{13}R = R\frac{(\delta_{CO_2} + 10^3)\Re_{V\text{-}PDB}}{(\delta_{CO_2} + 10^3)\Re_{V\text{-}PDB} + 10^3} \tag{18}$$

where δ_{CO_2} is the $\delta^{13}C$ of CO_2 produced from methane oxidation and $\Re_{V\text{-}PDB}$ is $^{13}C/^{12}C$ in the isotope reference standard. We neglect chemical and isotopic equilibration in the ΣCO_2 system because the reaction time for the conversion of CO_2(aq) to HCO_3^- ($\sim 10^1$ s; Zeebe and others, 1999) is long compared to the diffusion time for a distance characteristic of an archaea/SRB aggregate ($\sim 10^{-2}$ s).[12]

The equation for radial diffusion is undefined at $r = 0$; hence the inner boundary is offset a small distance (10 nm) from the true aggregate center. We assume that concentration gradients are zero near the center of the aggregate:

$$\frac{d[^{12}CO_2]}{dr} = \frac{d[^{13}CO_2]}{dr} = 0 \text{ at r} = 0.01\ \mu\text{m}. \tag{19}$$

The outer boundary is set at a distance of 10× the aggregate radius, and $[^{12}CO_2]$ and $[^{13}CO_2]$ are set to bulk porewater values calculated from porewater $[CO_2(aq)]$ and $\delta^{13}C\text{-}CO_2$ using equations analogous to (17) and (18). Equations (15) and (16) are solved by finite difference, and isotope ratios are expressed using standard δ-notation:

$$\delta^{13}C\text{-}CO_2 = \left[\frac{[^{13}CO_2]}{[^{12}CO_2]} - \Re_{V\text{-}PDB}\right]\frac{10^3}{\Re_{V\text{-}PDB}}. \tag{20}$$

We applied our model to sediments from Hydrate Ridge, where environmental conditions and archaea/SRB aggregate properties are well-characterized (table 4). The CO_2 production rate (R) in the archaeal portion of the aggregate was estimated using two approaches. In the first approach, we set R equal to the upper-limit rate of syntrophic methane oxidation to CO_2 and H_2 calculated from a diffusion-reaction model employing thermodynamic controls (fig. 5A, left panel; Alperin and Hoehler, 2009). The predicted CO_2(aq) concentration and $\delta^{13}C\text{-}CO_2$ profiles are shown by the solid vertical lines in figure 5A (middle and right panels, respectively). The isotope diffusion-reaction model predicts that micro-gradients in $\delta^{13}C\text{-}CO_2$ do exist, but they are not significant (CO_2 in the aggregate interior is "lighter" than the bulk porewater by only 0.00002‰). To illustrate that micro-gradients are possible when $Da > 1$, we reduced the molecular diffusion coefficient by seven orders-of-magnitude and re-ran

[10] O'Leary (1984) has shown that the ratio of diffusion coefficients for $^{12}CO_2$(aq) and $^{13}CO_2$(aq) is nearly one (1.0007 ± 0.0002).

[11] $D' = \varphi^3 D$ in fine-grained sediment (Ullman and Aller, 1982), whereas $D' = \eta D/\theta^2$ inside the aggregate. D is the molecular diffusion coefficient, φ is sediment porosity, θ is intracellular tortuosity related to obstacles in the cytoplasm, and η is a factor to account for elevated viscosity of the cytosol. In sediments where φ is 0.7, D is reduced by a factor of ~3; inside living cells, molecular crowding slows molecular diffusion by a factor or 2.3 (Dauty and Verkman, 2004) and elevated viscosity reduces D by an additional factor of ~1.5 (Dauty and Verkman, 2004; Stewart, 2003). Our conclusions are not affected by minor variations in D'.

[12] The diffusion time for length-scale ℓ is calculated as $\ell^2 D^{-1} = (3.2 \times 10^{-4}\ \text{cm})^2\ (4.6 \times 10^{-6}\ \text{cm}^2\ \text{s}^{-1})^{-1}$.

TABLE 4

Environmental conditions, archaea/SRB aggregate properties, and diffusion coefficient for CO_2(aq) in Hydrate Ridge sediments(1)

Bottom water temperature	4ºC (2)
Bottom water salinity	34 psu (3)
Water column depth	780 m (2)
Sediment porosity	0.65 (4)
Sediment pH	7.5 (5)
Porewater total alkalinity	21 meq L^{-1} (3)
Porewater [CO_2(aq)]	690 μM (6)
Porewater δ^{13}C-CO_2	–50 ‰ (7)
Porewater δ^{13}C-CH_4	–63 ‰ (7)
δ^{13}C of CO_2 produced from methane oxidation (δ_{CO_2})	–76 ‰ (8)
Sediment sulfate reduction rate	2500 μM d^{-1} (2)
Maximum aggregate abundance	6.7×10^7 cm^{-3} (2)
Diameter of aggregate	3.2 μm (2)
Diameter of archaeal inner sphere	2.3 μm (2)
Average CO_2 production rate in archaeal portion of aggregate	44 μM s^{-1} (9)
D' for CO_2(aq)	4.6×10^{-6} cm^2 s^{-1} (10)

(1) Sediment and porewater data are from the 1 to 2 cm depth interval at the southern Hydrate Ridge, mat-covered study site where Boetius and others (2000) report a distinct maximum in the abundance of archaea/SRB aggregates. (2) Boetius and others (2000). (3) Luff and Wallman (2003). (4) From *Beggiatoa*-field 2 (Treude and others, 2003). (5) Derived from a diagenetic model; measured pH values are biased by CO_2 degassing during core retrieval (Luff and Wallman, 2003). (6) Calculated from Total Alkalinity and pH at *in situ* temperature, salinity, and pressure using the program CO2SYS (Lewis and Wallace, 1998). (7) Table 1. (8) $\delta_{CO_2} \approx \delta(CH_4) - \varepsilon_{CH_4/CO_2} = -76‰$ (table 3). (9) If the sediment sulfate reduction rate (SRR) is coupled to archaeal methane oxidation, the average CO_2 production rate from methane oxidation (R) in the archaeal portion of the aggregate is:

$$R = \frac{3\varphi \cdot \mathrm{SRR}}{4\pi\rho_{Agg}(r_{Arch})^3}$$

where φ is sediment porosity, ρ_{Agg} is maximum aggregate abundance, and r_{Arch} is radius of the archaeal inner sphere in archaea/SRB aggregate. (10) $D' = \varphi^2 D$ (Ullman and Aller, 1982), where φ is sediment porosity and D is the molecular diffusion coefficient for CO_2(aq) at *in situ* temperature, salinity, and pressure (Boudreau, 1997).

the model. Although diffusive transport this slow is not possible in near-surface, unconsolidated sediments, this exercise shows that when the rate of CO_2 production dominates over diffusive mixing ($Da \sim 10^2$), SRB on the aggregate exterior could be exposed to methane-derived CO_2 that is highly depleted in ^{13}C relative to the porewater CO_2 pool.

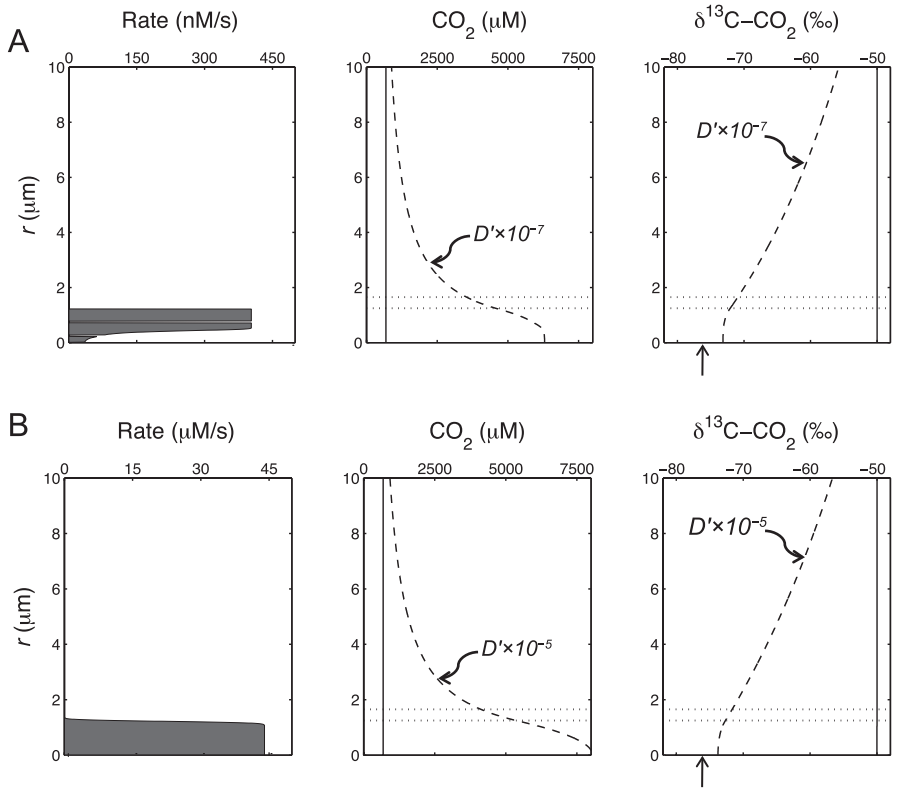

Fig. 5. CO_2(aq) concentration and δ^{13}C-CO_2 profiles in the vicinity of archaea/sulfate-reducing bacteria aggregates in Hydrate Ridge sediments calculated from an isotope diffusion-reaction model. The left panels show the CO_2 production rate in the archaeal portion of the aggregate estimated by two approaches: (A) a spherical diffusion-reaction model for methane oxidation to CO_2 and H_2 employing thermodynamic controls (Alperin and Hoehler, 2009); and (B) calculated from measurements of sediment sulfate-reduction rate, aggregate size, and abundance (table 4). The narrow gaps in CO_2 production in (A) reflect the restriction that methane oxidation does not occur in the cell wall and membrane (Alperin and Hoehler, 2009). Note that rates in (B) are 100× faster than in (A). The central and right panels show the predicted profiles for the best-estimate diffusion coefficient (solid, nearly vertical lines) and for diffusion coefficients reduced by factors of 10^7 (A) and 10^5 (B). Horizontal dotted lines delineate the archaeal and bacterial portions of the spherical aggregate. The vertical arrows in the right panels denote the isotopic composition of CO_2 produced by methane oxidation (table 4).

In the second approach, we use the measured sediment sulfate-reduction rate along with aggregate abundance and size (table 4) to estimate the aggregate-specific rate of CO_2 production (fig. 5B, left panel). These CO_2 production rates exceed the upper-limit rate (constrained by thermodynamics and physical transport) of syntrophic AMO involving interspecies H_2 transfer by two orders-of-magnitude (Alperin and Hoehler, 2009). Nevertheless, the predicted CO_2(aq) concentration and δ^{13}C-CO_2 profiles [shown by the solid vertical lines in fig. 5B (middle and right panels, respectively)] demonstrate that significant micro-gradients in δ^{13}C-CO_2 within an archaea/SRB aggregate are not possible.

CONCLUSIONS

The assumption that anaerobic methanotrophy is the most likely source of "ultra-light" ($\delta^{13}C < -60‰$) archaeal carbon in methane seep and hydrothermal vent sediments merits caution. At many of these sites, "ultra-light" carbon could be derived

from autotrophic methanogenesis. This finding may seem counter-intuitive because CO_2 tends to be isotopically "heavy" relative to methane in typical (non-seep/vent) methanogenic environments. However in seep/vent sediments, methane is isotopically "heavy" ($-35‰ \geq \delta^{13}C \geq -72‰$; table 1) compared to that found in typical marine sediments ($-50‰ \geq \delta^{13}C \geq -110‰$; Whiticar and others, 1986). At the same time, the sedimentary organic matter tends to be relatively "light" ($-27‰ \geq \delta^{13}C \geq -44‰$, excluding Guaymas Basin; table 1) due to the abundance of chemoautotrophic invertebrate communities, *Beggiatoa* mats, biomass derived from aerobic methanotrophy, and/or oil hydrocarbons (Sassen and others, 1993; Fisher, 1995; Joye and others, 2004; Niemann and others, 2006). Sulfate-reduction rates at methane seeps and hydrothermal vents are among the highest measured in marine sediments (Boetius and others, 2000; Weber and Jørgensen, 2002), and generate ΣCO_2 that isotopically resembles the organic matter. In addition, autotrophic methanogens utilize CO_2 (Fuchs and others, 1979; Vorholt and Thauer, 1997) that is depleted in ^{13}C by ~10 permil compared to ΣCO_2 (Zeebe and Wolf-Gladrow, 2001). As a result, the difference in $\delta^{13}C$ between CO_2 and methane (generally 20 to 30‰; table 1) is modest compared to the difference in kinetic isotope effects for CO_2 reduction and anaerobic methane oxidation [$\varepsilon_{CO_2/CH_4} - \varepsilon_{CH_4/CO_2} \approx 65‰$; eq (9) and table 3]. Since much of the fractionation between CO_2 and methane is retained in methanogen biomass [eq (8)], it is difficult to distinguish between anaerobic methanotrophy and autotrophic methanogenesis in methane seep and vent sediments solely on the basis of $\delta^{13}C$ values in cell carbon or lipids.

Furthermore, $\delta^{13}C$-CO_2 micro-gradients in archaea/SRB aggregates are not possible, and do not contribute to "ultra-light" carbon in SRB. Wegener and others (2008) have shown that ^{13}C is not incorporated into bacterial fatty acids in methane-seep sediments incubated with ^{13}C-CH_4, suggesting that the SRB do not assimilate methane or methane-derived intermediates such as acetate or formate. Autotrophic sulfate-reduction—without microgradients in $\delta^{13}C$-CO_2—provides a straightforward explanation for ^{13}C-depleted carbon in SRB (Londry and others, 2004) that is consistent with existing isotopic data and the constraints imposed by the physics of diffusion. The ability to use H_2 as an electron donor has been demonstrated in many genera of SRB, and numerous species are capable of autotrophic growth (Devereux and others, 1989). Wegener and others (2008) have shown that bacterial fatty acids attributed to SRB were labeled with ^{13}C when methane-seep sediments were incubated with ^{13}C-bicarbonate. Londry and others (2004) measured isotope effects for three species of SRB grown at 30 °C under autotrophic conditions. They report that biomass is depleted in ^{13}C relative to CO_2 by 10 to 29 permil, and lipids are depleted relative to biomass by 9 to 12 permil. If autotrophic sulfate-reduction occurs in sediments from Eel River Basin where $\delta(CO_2)$ is -38 permil (table 1), and if the isotope effects from Londry and others are pertinent, we predict $\delta^{13}C$ values for biomass of -48 to -67 permil and lipids of -57 to -79 permil. These predicted values overlap with measurements: bacterial cells in the outer layer of archaea/SRB aggregates have a $\delta^{13}C$ of -62 permil (Orphan and others, 2001b); non-isoprenoidal ether lipids attributed to the bacterial members of the aggregate have $\delta^{13}C$ values of -64 to -92 permil (Hinrichs and others, 2000).

It is common practice to classify an organism as an "ANME" (acronym for ANaerobic MEthanotroph) if its 16S ribosomal rRNA gene is monophyletic with the methanogen-like 16S rRNA recovered from methane-seep sediments containing ^{13}C-depleted ($\delta^{13}C < -60‰$) archaeal lipids. Given the ambiguity of the isotopic constraint, we recommend that the term "ANME" be replaced by "MLA" (Methanogen-Like Archaea) to account for uncertainty in the metabolic processes that are mediated by these archaea and to reflect their genetic similarity to methanogens.

ACKNOWLEDGMENTS

John Hayes and Ketil Sørensen reviewed an earlier version of this paper and their comments and suggestions were invaluable. We thank John Kessler, Karen Lloyd, Christof Meile, and Jack Middelburg for their constructive reviews. Don Canfield called our attention to the need to consider reversibility in the reaction network for methanogenesis. This research was supported by a grant from the National Science Foundation (OCE-00032358).

Appendix

The first five reactions in the biochemical pathway for methane production from CO_2 and H_2 (CO_2 to CH_3—H_4MPT; fig. 1) are reversible (Thauer and others, 1993):

$$\mathrm{CO_2} \underset{\varepsilon_{ba},\,\varphi_{ba}}{\overset{\varepsilon_{ab},\,\varphi_{ab}\quad \delta_{(B)}}{\rightleftharpoons}} \mathrm{CHO{-}MFR} \underset{\varepsilon_{cb},\,\varphi_{cb}}{\overset{\varepsilon_{bc},\,\varphi_{bc}\quad \delta_{(C)}}{\rightleftharpoons}} \mathrm{CHO{-}H_4MPT} \underset{\varepsilon_{dc},\,\varphi_{dc}}{\overset{\varepsilon_{cd},\,\varphi_{cd}}{\rightleftharpoons}}$$

$$\mathrm{CH^{+}{\equiv}H_4MPT} \underset{\varepsilon_{cd},\,\varphi_{cd}}{\overset{\varepsilon_{dc},\,\varphi_{dc}\quad \delta_{(E)}}{\rightleftharpoons}} \mathrm{CH_2{=}H_4MPT} \underset{\varepsilon_{fc},\,\varphi_{fc}}{\overset{\varepsilon_{cf},\,\varphi_{cf}\quad \delta_{(F)}}{\rightleftharpoons}} \mathrm{CH_3{-}H_4MPT} \xrightarrow{\overline{\varepsilon_f},\,\delta_f,\,\varphi_f} \ldots \quad \text{(A1)}$$

where $\delta(I)$ is the $\delta^{13}C$ of the CO_2-derived carbon in intermediate I, ε_{ij} and φ_{if} represent the isotope effect and mass flux, respectively, for the forward reaction ($I \rightarrow J$), ε_{ji} and φ_{ji} are the isotope effect and flux for the reverse reaction ($I \leftarrow J$), $\overline{\varepsilon_f}$ is the average isotope effect for forward reactions involving CH_3—H_4MPT, and δ_f and φ_f denote the isotopic composition and flux, respectively, of the carbon (originally derived from CO_2) that is transmitted downstream from CH_3—H_4MPT. Chemical abbreviations in (A1) are defined in the caption to figure 1.

Rees (1973) derived a steady-state, mass-balance expression for the overall isotope effect arising from a series of reversible, non-branching reactions. Applying his expression to the reactions in (A1), the overall isotope effect (ε_{af}) is:

$$\varepsilon_{af} \approx \varepsilon_{ab} + (\varepsilon_{bc} - \varepsilon_{ba})X_b + (\varepsilon_{cd} - \varepsilon_{cb})X_bX_c + (\varepsilon_{de} - \varepsilon_{dc})X_bX_cX_d + (\varepsilon_{ef} - \varepsilon_{ed})X_bX_cX_dX_e + (\overline{\varepsilon_f} - \varepsilon_{fe})X_bX_cX_dX_eX_f \quad \text{(A2)}$$

where $X_j\left(\equiv \dfrac{\varphi_{ji}}{\varphi_{ij}}\right)$ is the ratio of reverse flux to forward flux.[13] For the sake of brevity, let

$$\varepsilon' = (\varepsilon_{bc} - \varepsilon_{ba}) + (\varepsilon_{cd} - \varepsilon_{cb})X_c + (\varepsilon_{de} - \varepsilon_{dc})X_cX_d + (\varepsilon_{ef} - \varepsilon_{ed})X_cX_dX_e + (\overline{\varepsilon_f} - \varepsilon_{fe})X_cX_dX_eX_f. \quad \text{(A3)}$$

Combining equations (A2) and (A3), the overall isotope effect for the first five reversible steps of the CO_2-reduction pathway is given by:

$$\varepsilon_{af} \approx \varepsilon_{ab} + X_b\varepsilon'. \quad \text{(A4)}$$

Given that $\varepsilon_{af} \approx \delta(CO_2) - \delta_f$ (see footnote 1 in main text):

$$\delta_f \approx \delta(CO_2) - (\varepsilon_{ab} + X_b\varepsilon'). \quad \text{(A5)}$$

The final two reactions in the dissimilatory pathway (CH_3—H_4MPT $\rightarrow$ CH_3—S—CoM and CH_3—S—CoM $\rightarrow$ CH_4; fig. 1) are thought to be irreversible (Gärtner and others, 1994; Thauer 1998), whereas the anabolic reaction at the assimilation-dissimilation branch point (CH_3—H_4MPT $\rightleftarrows$ CH_3—CO—S—CoA) is probably reversible since acetoclastic methanogens use this pathway to convert acetate to methane (Thauer, 1998):

[13] Equation (A2) is written as an approximation because it assumes that $^{12}C + {}^{13}C \approx {}^{12}C$ (Rees, 1973).

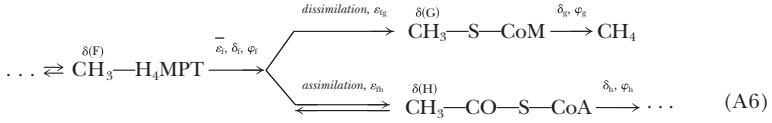

(A6)

where δ_g, φ_g and δ_h, φ_h denote the $\delta^{13}C$ and flux of transmitted carbon derived from the methyl-group in CH_3—S—CoM and CH_3—CO—S—CoA, respectively. Assuming that anabolic reactions following CH_3—CO—S—CoA production are unidirectional, and that $\varphi_f = \varphi_g + \varphi_h$, the steady-state mass-balance equation for ^{13}C at the assimilation-dissimilation branch point is:

$$\delta_f = (1 - f_h)\delta_g + f_h\delta_h, \tag{A7}$$

where the branching ratio (f_h) is defined as $\frac{\varphi_h}{\varphi_f}$ and $(1 - f_h) = \frac{\varphi_g}{\varphi_f}$.

Given that $\varepsilon_{fg} \approx \delta(F) - \delta_g$ and $\varepsilon_{fh} \approx \delta(F) - \delta_h$ (see footnote 1 in main text) and defining $\Delta\varepsilon$ ($\equiv \varepsilon_{fh} - \varepsilon_{fg}$) as the net isotope effect at the assimilation-dissimilation branch-point:

$$\delta_h = \delta_g - \Delta\varepsilon. \tag{A8}$$

From equations (A7) and (A8),

$$\delta_f = (1 - f_h)\delta_g + f_h(\delta_g - \Delta\varepsilon) \tag{A9}$$

which simplifies to:

$$\delta_g = \delta_f + f_h\Delta\varepsilon. \tag{A10}$$

Since the $\delta^{13}C$ of methane produced by CO_2 reduction, $\delta(CH_4)$, must equal δ_g, and combining equations (A5) and (A10):

$$\delta(CH_4) \approx \delta(CO_2) - (\varepsilon_{ab} + X_b\varepsilon') + f_h\Delta\varepsilon. \tag{A11 or 1}$$

Likewise, combining equations (A8) and (A11), and substituting δ_g for $\delta(CH_4)$:

$$\delta_h \approx \delta(CO_2) - (\varepsilon_{ab} + X_b\varepsilon') - (1 - f_h)\Delta\varepsilon. \tag{A12 or 3}$$

References

Alperin, M. J., and Hoehler, T. M., 2009, Anaerobic methane oxidation by archaea/sulfate-reducing bacteria aggregates: 1. Thermodynamic and physical constraints: American Journal of Science, v. 309, p. 869–957, doi:10.2475/10.2009.01.

Alperin, M. J., Reeburgh, W. S., and Whiticar, M. J., 1988, Carbon and hydrogen isotope fractionation resulting from anaerobic methane oxidation: Global Biogeochemical Cycles, v. 2, p. 279–288, doi: 10.1029/GB002i003p00279.

Alperin, M. J., Blair, N. E., Albert, D. B., Hoehler, T. M., and Martens, C. S., 1992, Factors that control the stable carbon isotopic composition of methane produced in an anoxic marine sediment: Global Biogeochemical Cycles, v. 6, p. 271–291, doi:10.1029/92GB01650.

Balabane, M., Galimov, E., Hermann, M., and Létolle, R., 1987, Hydrogen and carbon isotope fractionation during experimental production of bacterial methane: Organic Geochemistry, v. 11, p. 115–119, doi:10.1016/0146-6380(87)90033-7.

Baresi, L., Alperin, M., Bullister, J., Giani, D., Harvey, H. R., Kuivila, K., and Slock, J., 1983, Ecology of methanogenesis: Distribution, physiology, and carbon stable-isotope fractionation, *in* Margulis, L., Nealson, K. H., and Taylor, I., editors, Planetary biology and microbial ecology: Biochemistry of carbon and early life: National Aeronautics and Space Administration, Technical Memorandum 86043, p. 81–122.

Belyaev, S. S., Wolkin, R., Kenealy, W. R., DeNiro, M. J., Epstein, S., and Zeikus, J. G., 1983, Methanogenic bacteria from the Bondyuzhskoe oil field: general characterization and analysis of stable-carbon isotopic fractionation: Applied and Environmental Microbiology, v. 45, p. 691–697.

Berner, R. A., 1980, Early diagenesis, a theoretical approach: Princeton, New Jersey, Princeton University Press, 241 p.

Bian, L., Hinrichs, K.-H., Xie, T., Brassell, S. C., Iversen, N., Fossing, H., Jørgensen, B. B., and Hayes, J. M., 2001, Algal and archaeal polyisoprenoids in a recent marine sediment: Molecular-isotopic evidence for anaerobic methane oxidation: Geochemistry, Geophysics, Geosystems, v. 2, 1023, doi:10.1029/2000GC000112.

Boetius, A., Ravenschlag, K., Schubert, C. J., Rickert, D., Widdel, F., Gieseke, A., Amann, R., Jørgensen, B. B., Witte, U., and Pfankuche, O., 2000, A marine microbial consortium apparently mediating anaerobic oxidation of methane: Nature, v. 407, p. 623–626, doi:10.1038/35036572.

Botz, R., Pokojski, H.-D., Schmitt, M., and Thomm, M., 1996, Carbon isotope fractionation during bacterial methanogenesis by CO_2 reduction: Organic Geochemistry, v. 25, p. 255–262, doi:10.1016/S0146-6380(96)00129-5.

Boudreau, B. P., 1997, Diagenetic models and their implementation: Modelling transport and reactions in aquatic sediments: Heidelberg, Springer, 414 p.

Crank, J., 1975, The mathematics of diffusion: New York, Oxford University Press, 414 p.

Dauty, E., and Verkman, A. S., 2004, Molecular crowding reduces to a similar extent the diffusion of small solutes and macromolecules: measurement by fluorescence correlation spectroscopy: Journal of Molecular Recognition, v. 17, p. 441–447, doi:10.1002/jmr.709.

Devereux, R., Delaney, M., Widdel, F., and Stahl, D. A., 1989, Natural relationships among sulfate-reducing eubacteria: Journal of Bacteriology, v. 171, p. 6689–6695.

Duan, Z., Møller, N., Greenberg, J., and Weare, J. H., 1992, The prediction of methane solubility in natural waters to high ionic strength from 0 to 250°C and from 0 to 1600 bar: Geochimica et Cosmochimica Acta, v. 56, p. 1451–1460, doi:10.1016/0016-7037(92)90215-5.

Elvert, M., Suess, E., and Whiticar, M. J., 1999, Anaerobic methane oxidation associated with marine gas hydrates: superlight C-isotopes from saturated and unsaturated C20 and C25 irregular isoprenoids: Naturwissenschaften, v. 86, p. 295–300, doi:10.1007/s001140050619.

Elvert, M., Suess, E., Greinert, J., and Whiticar, M. J., 2000, Archaea mediating anaerobic methane oxidation in deep-sea sediments at cold seeps of the eastern Aleutian subduction zone: Organic Geochemistry, v. 31, p. 1175–1187, doi:10.1016/S0146-6380(00)00111-X.

Elvert, M., Greinert, J., Suess, E., and Whiticar, M. J., 2001, Carbon isotopes of biomarkers derived from methane-oxidizing microbes at Hydrate Ridge, Cascadia convergent margin, *in* Paull, C. K., and Dillon, W. P., editors, Natural gas hydrates: occurrence, distribution, and detection: American Geophysical Union, Geophysical Monograph 124, p. 115–129.

Fisher, C. R., 1995, Toward an appreciation of hydrothermal-vent animals: their environment, physiological ecology, and tissue stable isotope values, *in* Humphris, S. E., Zierenberg, R. A., Mullineaux, L. S., and Thomson, R. E., editors, Seafloor Hydrothermal Systems: Physical, Chemical, Biological, and Geochemical: American Geophysical Union, Geophysical Monograph 91, p. 297–316.

Fuchs, G., Thauer, R., Ziegler, H., and Stichler, W., 1979, Carbon isotope fractionation by *Methanobacterium thermoautotrophicum:* Archives of Microbiology, v. 120, p. 135–139, doi:10.1007/BF00409099.

Games, L. M., and Hayes, J. M., 1976, On the mechanisms of CO_2 and CH_4 production in natural anaerobic environments, *in* Nriagu, J. O., editor, Proceedings of the Second International Symposium on Environmental Biogeochemistry: Ann Arbor, Michigan, Science Press, p. 51–73.

Games, L. M., Hayes, J. M., and Gunsalus, R. P., 1978, Methane-producing bacteria: natural fractionations of the stable carbon isotopes: Geochimica et Cosmochimica Acta, v. 42, p. 1295–1297, doi:10.1016/0016-7037(78)90123-0.

Gärtner, P., Weiss, D. S., Harms, U., and Thauer, R. K., 1994, N^5-Methyltetrahydromethan-opterin: Coenzyme M methyltransferase from *Methanobacterium thermoautotrophicum*, Catalytic mechanism and sodium ion dependence: European Journal of Biochemistry, v. 226, p. 465–472, doi:10.1111/j.1432-1033.1994.tb20071.x.

Grossman, E. L., Cifuentes, L. A., and Cozzarelli, I. M., 2002, Anaerobic methane oxidation in a landfill-leachate plume: Environmental Science and Technology, v. 36, p. 2436–2442, doi:10.1021/es015695y.

Haese, R. R., Meile, C., Van Cappellen, P., and De Lange, G. J., 2003, Carbon geochemistry of cold seeps: Methane fluxes and transformation in sediments from Kazan mud volcano, eastern Mediterranean Sea: Earth and Planetary Science Letters, v. 212, p. 361–375, doi:10.1016/S0012-821X(03)00226-7.

Hayes, J. M., 1993, Factors controlling ^{13}C contents of sedimentary organic compounds: Principles and evidence: Marine Geology, v. 113, p. 111–125, doi:10.1016/0025-3227(93)90153-M.

Hayes, J. M., 2001, Fractionation of Carbon and Hydrogen Isotope in Biosynthetic Processes, *in* Valley, J. W., and Cole, D. R., editors, Stable Isotope Geochemistry: Reviews in Mineralogy and Geochemistry, v. 43, p. 225–277, doi:10.2138/gsrmg.43.1.225.

Hinrichs, K.-U., and Boetius, A., 2002, The anaerobic oxidation of methane: New insights in microbial ecology and biogeochemistry, *in* Wefer, G., Billett, D., Jørgensen, B. B., Schlüter, M., and Van Weering, T., editors, Ocean Margin Systems: New York, Springer-Verlag, p. 457–477.

Hinrichs, K.-U., Hayes, J. M., Sylva, S. P., Brewer, P. G., and DeLong, E. F., 1999, Methane-consuming archaebacteria in marine sediments: Nature, v. 398, p. 802–805, doi:10.1038/19751.

Hinrichs, K.-U., Summons, R. E., Orphan, V., Sylva, S. P., and Hayes, J. M., 2000, Molecular and isotopic analysis of anaerobic methane-oxidizing communities in marine sediments: Organic Geochemistry, v. 31, p. 1685–1701, doi:10.1016/S0146-6380(00)00106-6.

Hoehler, T. M., Alperin, M. J., Albert, D. B., and Martens, C. S., 1994, Field and laboratory studies of methane oxidation in an anoxic marine sediment: evidence for a methanogen-sulfate reducer consortium: Global Biogeochemical Cycles, v. 8, p. 451–463, doi:10.1029/94GB01800.

Holler, T., Wegener, G., Knittel, K., Boetius, A., Brunner, B., Kuypers, M. M. M., and Widdel, F., 2009, Substantial $^{13}C/^{12}C$ and D/H fractionation during anaerobic oxidation of methane by marine consortia enriched *in vitro*: Environmental Microbiology Reports, v. 1, p. 370–376, doi:10.1111/j.1758-2229.2009.00074.x.

House, C. H., Schopf, J. W., and Stetter, K. O., 2003, Carbon isotopic fractionation by Archaeans and other thermophilic prokaryotes: Organic Geochemistry, v. 34, p. 345–356, doi:10.1016/S0146-6380(02)00237-1.

Huskey, W. P., 1991, Origins and interpretations of heavy-atom isotope effects, *in* Cook, P. F., editor, Enzyme mechanism from isotope effects: Boca Raton, Ann Harbor, London, CRC Press, p. 37–72.

Iversen, N., and Jørgensen, B. B., 1985, Anaerobic methane oxidation rates at the sulfate-methane transition in marine sediments from Kattegat and Skagerrak (Denmark): Limnology and Oceanography, v. 30, p. 944–955.

Joye, S. B., Boetius, A., Orcutt, B. N., Montoya, J. P., Schulz, H. N., Erickson, M. J., and Lugo, S. K., 2004, The anaerobic oxidation of methane and sulfate reduction in sediments from Gulf of Mexico cold seeps: Chemical Geology, v. 205, p. 219–238, doi:10.1016/j.chemgeo.2003.12.019.

Kessler, J. D., Reeburgh, W. S., and Tyler, S. C., 2006, Controls on methane concentration and stable isotope (δ^2H-CH_4 and δ^{13}C-CH_4) distributions in the water columns of the Black Sea and Cariaco Basin: Global Biogeochemical Cycles, v. 20, 10.1029/2005GB002571.

Laier, T., Kuijpers, A., Dennegård, B., and Heier-Nielsen, S., 1996, Origin of shallow gas in Skagerrak and Kattegat—evidence from stable isotopic analyses and radiocarbon dating: NGU (Geological Survey of Norway) Bulletin, v. 430, p. 129–136.

Lerman, A., 1979, Geochemical processes: Water and sediment environments: New York, Wiley-Interscience, 481 p.

Lewis, E., and Wallace, D. W. R., 1998, Program developed for CO_2 system calculations: Oak Ridge, Tennessee, U.S. Department of Energy, Oak Ridge National Laboratory, ORNL/CDIAC-105, Carbon Dioxide Information Analysis Center.

Londry, K. L., Jahnke, L. L., and Des Marais, D. J., 2004, Stable carbon isotope ratios of lipid biomarkers of sulfate-reducing bacteria: Applied and Environmental Microbiology, v. 70, p. 745–751, doi:10.1128/AEM.70.2.745-751.2004.

Londry, K. L., Dawson, K. G., Grover, H. D., Summons, R. E., and Bradley, A. S., 2008, Stable carbon isotope fractionation between substrates and products of *Methanosarcina barkeri:* Organic Geochemistry, v. 39, p. 608–621, doi:10.1016/j.orggeochem.2008.03.002.

Luff, R., and Wallman, K., 2003, Fluid flow, methane fluxes, carbonate precipitation and biogeochemical turnover in gas hydrate-bearing sediments at Hydrate Ridge, Cascadia Margin: Numerical modeling and mass balances: Geochimica et Cosmochimica Acta, v. 67, p. 3403–3421, doi:10.1016/S0016-7037(03)00127-3.

Martens, C. S., Albert, D. B., and Alperin, M. J., 1999, Stable isotope tracing of anaerobic methane oxidation in the gassy sediments of Eckernförde Bay, German Baltic Sea: American Journal of Science, v. 299, p. 589–610, doi:10.2475/ajs.299.7-9.589.

MEDINAUT/MEDINETH Shipboard Parties, 2000, Linking Mediterranean brine pools and mud volcanism: Eos, v. 81, p. 625, 631–632.

Michaelis, W., Seifert, R., Nauhaus, K., Treude, T., Thiel, V., Blumenberg, M., Knittel, K., Gieseke, A., Peterknecht, K., Pape T., Boetius, A., Amann, R., Jørgensen, B. B., Widdel, F., Peckmann, J., Pimenov, N. V., and Gulin, M. B., 2002, Microbial reefs in the Black Sea fueled by anaerobic oxidation of methane: Science, v. 297, p. 1013–1015, doi:10.1126/science.1072502.

Niemann, H., Lösekann, T., de Beer, D., Elvert, M., Nadalig, T., Knittel, K., Amann, R., Sauter, E. J., Schlüter, M., Klages, M., Foucher, J. P., and Boetius, A., 2006, Novel microbial communities of the Haakon Mosby mud volcano and their role as a methane sink: Nature, v. 443, p. 854–858, doi:10.1038/nature05227.

O'Leary, M. H., 1980, Determination of heavy-atom isotope effects on enzyme-catalyzed reactions: Methods in Enzymology, v. 64, p. 83–104, doi:10.1016/S0076-6879(80)64006-3.

——— 1984, Measurement of the isotope fractionation associated with diffusion of carbon dioxide in aqueous solution: Journal of Physical Chemistry, v. 88, p. 823–825, doi:10.1021/j150648a041.

Orphan, V. J., Hinrichs, K.-U., Ussler III, W., Paull, C. K., Taylor, L. T., Sylva, S. P., Hayes, J. M., and DeLong, E. F., 2001a, Comparative analysis of methane-oxidizing archaea and sulfate-reducing bacteria in anoxic marine sediments: Applied and Environmental Microbiology, v. 67, p. 1922–1034, doi:10.1128/AEM.67.4.1922-1934.2001.

Orphan, V. J., House, C. H., Hinrichs, K.-U., McKeegan, K. D., and DeLong, E. F., 2001b, Methane-consuming archaea revealed by directly coupled isotopic and phylogenetic analysis: Science, v. 293, p. 484–487, doi:10.1126/science.1061338.

——— 2002, Multiple archaeal groups mediate methane oxidation in anoxic cold seep sediments: Proceedings of the National Academy of Sciences, v. 99, p. 7663–7668, doi:10.1073/pnas.072210299.

Pancost, R. D., Sinninghe Damsté, J. S., de Lint, S., van der Maarel, M. J. E. C., Gottschal, J. C., and The Medinaut Shipboard Scientific Party, 2000, Biomarker evidence for widespread anaerobic methane oxidation in Mediterranean sediments by a consortium of methanogenic archaea and bacteria: Applied and Environmental Microbiology, v. 66, p. 1126–1132, doi:10.1128/AEM.66.3.1126-1132.2000.

Pancost, R. D., Hopmans, E. C., Sinninghe Damsté, J. S., and The Medinaut Shipboard Scientific Party, 2001, Archaeal lipids in Mediterranean cold seeps: molecular proxies for anaerobic methane oxidation: Geochimica et Cosmochimica Acta, v. 65, p. 1611–1627, doi:10.1016/S0016-7037(00)00562-7.

Penning, H., Plugge, C. M., Galand, P. E., and Conrad, R., 2005, Variation of carbon isotope fractionation in hydrogenotrophic methanogenic microbial cultures and environmental samples at different energy status: Global Change Biology, v. 11, p. 2103–2113, doi:10.1111/j.1365-2486.2005.01076.x.

Peter, J. M., and Shanks III, W. C., 1992, Sulfur, carbon, and oxygen isotope variations in submarine hydrothermal deposits of Guaymas Basin, Gulf of California, USA: Geochimica et Cosmochimica Acta, v. 56, p. 2025–2040, doi:10.1016/0016-7037(92)90327-F.

Reeburgh, W. S., 1980, Anaerobic methane oxidation: Rate depth distributions in Skan Bay sediments: Earth and Planetary Science Letters, v. 47, p. 345–352, doi:10.1016/0012-821X(80)90021-7.

——— 2003, Global methane biogeochemistry, *in* Keeling, R. F., editor, The Atmosphere: Elsevier-Pergamon, Treatise on Geochemistry, v. 4, p. 1–32, doi:10.1016/B0-08-043751-6/04036-6.

Rees, C. E., 1973, A steady-state model for sulphur isotope fractionation in bacterial reduction processes: Geochimica et Cosmochimica Acta, v. 37, p. 1141–1162, doi:10.1016/0016-7037(73)90052-5.

Richet, P., Bottinga, Y., and Javoy, M., 1977, A review of hydrogen, carbon, nitrogen, oxygen, sulphur, and chlorine stable isotope fractionation among gaseous molecules: Annual Review of Earth and Planetary Science Letters, v. 5, p. 65–110, doi:10.1146/annurev.ea.05.050177.000433.

Roberts, H. H., 2001, Fluid and gas expulsion on the northern Gulf of Mexico continental slope: Mud-prone to mineral-prone responses, *in* Paull, C. K., and Dillon, W. P., editors, Natural gas hydrates: Occurrences, Distribution, and Detection: American Geophysical Union, Geophysical Monograph 124, p. 145–161.

Sahores, J. J., and Witherspoon, P. A., 1970, Diffusion of light paraffin hydrocarbons in water from 2°C to 80°C, *in* Hobson, G. D., and Spears, G. C., editor, Advances in Organic Geochemistry, 1966: New York, Pergamon, p. 219–230.

Sassen, R., Roberts, H. H., Aharon, P., Larkin, J., Chinn, E. W., and Carney, R., 1993, Chemosynthetic bacterial mats at cold hydrocarbon seeps, Gulf of Mexico continental slope: Organic Geochemistry, v. 20, p. 77–89, doi:10.1016/0146-6380(93)90083-N.

Sassen, R., Joye, S., Sweet, S. T., DeFreitas, D. A., Milkov, A. V., and MacDonald, I. R., 1999, Thermogenic gas hydrates and hydrocarbon gases in complex chemosynthetic communities, Gulf of Mexico continental slope: Organic Geochemistry, v. 30, p. 485–497, doi:10.1016/S0146-6380(99)00050-9.

Simpson, P. G., and Whitman, W. B., 1993, Anabolic pathways in methanogens, *in* Ferry, J. G., editor, Methanogenesis: ecology, physiology, biochemistry, and genetics: New York, Chapman and Hall, p. 445–472.

Stewart, P. S., 2003, Diffusion in biofilms: Journal of Bacteriology, v. 185, p. 1485–1491, doi:10.1128/JB.185.5.1485-1491.2003.

Suess, E., Bohrmann, G., von Huene, R., Linke, P., Wallman, K., Lammers, S., Sahling, H., Lutz, R. A., and Orange, D., 1998, Fluid venting in the eastern Aleutian subduction zone: Journal of Geophysical Research-Solid Earth, v. 103, n. B2, p. 2597–2614, doi:10.1029/97JB02131.

Summons, R. E., Franzmann, P. D., and Nichols, P. D., 1998, Carbon isotopic fractionation associated with methylotrophic methanogenesis: Organic Geochemistry, v. 28, p. 465–475, doi:10.1016/S0146-6380(98)00011-4.

Takigiku, R., ms, 1987, Isotopic and molecular indicators of origins of organic compounds in sediments: Bloomington, Indiana, Indiana Univeristy, Ph. D. thesis, 248 p.

Teske, A., Hinrichs, K.-U., Edgecomb, V., de Vera Gomez, A., Kysela, D., Sylva, S. P., Sogin, M. L., and Jannasch, H. W., 2002, Microbial diversity of hydrothermal sediments in the Guaymas Basin: Evidence for anaerobic methanotrophic communities: Applied and Environmental Microbiology, v. 68, p. 1994–2007, doi:10.1128/AEM.68.4.1994-2007.2002.

Thauer, R. K., 1998, Biochemistry of methanogenesis: a tribute to Marjory Stephenson: Microbiology, v. 144, p. 2377–2406, doi:10.1099/00221287-144-9-2377.

Thauer, R. K., Hedderich, R., and Fisher, R., 1993, Reactions and enzymes involved in methanogenesis from CO_2 and H_2, *in* Ferry, J. G., editor, Methanogenesis: ecology, physiology, biochemistry, and genetics: New York, Chapman and Hall, p. 209–252.

Thiel, V., Peckmann, J., Richnow, H. H., Luth, U., Reitner, J., and Michaelis, W., 2001, Molecular signals for anaerobic methane oxidation in Black Sea seep carbonates and a microbial mat: Marine Chemistry, v. 73, p. 97–112, doi:10.1016/S0304-4203(00)00099-2.

Thomsen, T. R., Finster, K., and Ramsing, N. B., 2001, Biogeochemical and molecular signatures of anaerobic methane oxidation in a marine sediment: Applied and Environmental Microbiology, v. 67, p. 1646–1656, doi:10.1128/AEM.67.4.1646-1656.2001.

Treude, T., Boetius, A., Knittel, K., Wallman, K., and Jørgensen, B. B., 2003, Anaerobic oxidation of methane above gas hydrates at Hydrate Ridge, NE Pacific ocean: Marine Ecology Progress Series, v. 264, p. 1–14, doi:10.3354/meps264001.

Ullman, W. J., and Aller, R. C., 1982, Diffusion coefficients in nearshore marine sediments: Limnology and Oceanography, v. 27, p. 552–556.

Valentine, D. L., Chidthaisong, A., Rice, A., Reeburgh, W. S., and Tyler, S. C., 2004, Carbon and hydrogen isotope fractionation by moderately thermophilic methanogens: Geochimica et Cosmochimica Acta, v. 68, p. 1571–1590, doi:10.1016/j.gca.2003.10.012.

Valentine, D. L., Kastner, M., Wardlaw, G. D., Wang, X., Purdy, A., and Bartlett, D. H., 2005, Biogeochemical investigations of marine methane seeps, Hydrate Ridge, Oregon: Journal of Geophysical Research, v. 110, G02005, doi:10.1029/2005JG000025.

Vorholt, J. A., and Thauer, R. K., 1997, The active species of "CO_2" utilized by formylmethanofuran dehydrogenase from methanogenic Archaea: European Journal of Biochemistry, v. 248, p. 919–924, doi:10.1111/j.1432-1033.1997.00919.x.

Weber, A., and Jørgensen, B. B., 2002, Bacterial sulfate reduction in hydrothermal sediments of the Guaymas Basin, Gulf of California, Mexico: Deep-Sea Research Part I: Oceanographic Research Papers, v. 49, p. 827–841, doi:10.1016/S0967-0637(01)00079-6.

Weber, A., Riess, W., Wenzhoefer, F., and Jørgensen, B. B., 2001, Sulfate reduction in Black Sea sediments: in situ and laboratory radiotracer measurements from the shelf to 2000 m depth: Deep-sea Research Part I: Oceanographic Research Papers, v. 48, p. 2073–2096, doi:10.1016/S0967-0637(01)00006-1.

Wegener, G., Niemann, H., Elvert, M., Henrichs, K.-U., and Boetius, A., 2008, Assimilation of methane and inorganic carbon by microbial communities mediating the anaerobic oxidation of methane: Environmental Microbiology, v. 10, p. 2287–2298, doi:10.1111/j.1462-2920.2008.01653.x.

Weiss, P. M., 1991, Heavy atom isotope effects using the isotope ratio mass spectrometer, *in* Cook, P. F., editor, Enzyme mechanism from isotope effects: Boca Raton, Florida, CRC Press, p. 291–312.

Werne, J. P., Baas, M., and Sinninghe Damsté, J. S., 2002, Molecular isotopic tracing of carbon flow and trophic relationships in a methane-supported benthic microbial community: Limnology and Oceanography, v. 47, p. 1694–1701.

Whiticar, M. J., 1999, Carbon and hydrogen isotope systematics of bacterial formation and oxidation of methane: Chemical Geology, v. 161, p. 291–314, doi:10.1016/S0009-2541(99)00092-3.

Whiticar, M. J., and Faber, E., 1986, Methane oxidation in sediment and water column environments—Isotope evidence: Organic Geochemistry, v. 10, p. 759–768, doi:10.1016/S0146-6380(86)80013-4.

Whiticar, M. J., Faber, E., and Schoell, M., 1986, Biogenic methane formation in marine and freshwater environments: CO_2 reduction vs. acetate fermentation—Isotope evidence: Geochimica et Cosmochimica Acta, v. 50, p. 693–709, doi:10.1016/0016-7037(86)90346-7.

Zeebe, R. E., and Wolf-Gladrow, D., 2001, CO_2 in seawater: equilibrium, kinetics, isotopes: Elsevier Oceanography Series, 65, 346 p.

Zeebe, R. E., Wolf-Gladrow, D. A, and Jansen, H., 1999, On the time required to establish chemical and isotopic equilibrium in the carbon dioxide system in seawater: Marine Chemistry, v. 65, p. 135–153, doi:10.1016/S0304-4203(98)00092-9.

Zhang, J., Quay, P. D., and Wilbur, D. O., 1995, Carbon isotope fractionation during gas-water exchange and dissolution of CO_2: Geochimica et Cosmochimica Acta, v. 59, p. 107–114, doi:10.1016/0016-7037(95)91550-D.

Zhang, C. L., Li, Y., Wall, J. D., Larsen, L., Sassen, R., Huang, Y., Wang, Y., Peacock, A., White, D. C., Horita, J., and Cole, D. R., 2002, Lipid and carbon isotopic evidence of methane-oxidizing and sulfate-reducing bacteria in association with gas hydrates from the Gulf of Mexico: Geology, v. 30, p. 239–242, doi:10.1130/0091-7613(2002)030⟨0239:LACIEO⟩2.0.CO;2.

Zhang, C. L., Pancost, R. D., Sassen, R., Qian, Y., and Macko, S. A., 2003, Archaeal lipid biomarkers and isotopic evidence of anaerobic methane oxidation associated with gas hydrates in the Gulf of Mexico: Organic Geochemistry, v. 34, p. 827–836, doi:10.1016/S0146-6380(03)00003-2.